Table 1 Features of Medicaid personal care services male clients aged 65+ by depressive symptoms

Full sample (M11Q) $n = 200$	No depressive symptoms $n = 179$ (89.5%)	Depressive symptoms $n = 21$ (10.5%)
Demographics		
Age ± SD (years)	78.92 ± 7.66	81.10 ± 7.38
Personal care services		
Hours/week (mean ± SD)	54.40 ± 44.45	61.76 ± 47.85
Duration, years (mean ± SD)	7.60 ± 5.75	4.95 ± 3.29*
Medical status		
Number of diseases (mean ± SD)	5.01 ± 1.35	5.58 ± 1.63
Cognitive impairment		
No impairment, %	36.5	14.3
Dementia, %	63.5	85.7
Functional status		
Number of ADL disabilities (mean ± SD)	3.92 ± 1.66	4.33 ± 1.77
Sensory impairment		
Speech impairment, %	29.2	42.9
Visual impairment, %	44.9	66.7*
Hearing impairment, %	43.3	76.2**
Muscular impairment		
Dominant hand/arm impairment, %	29.2	40.0
Upper extremities impairment, %	43.8	70.0*
Lower extremities impairment, %	71.8	80.0
Bladder incontinence, %	38.8	65.0*
Socio-environmental status		
Living situation		
Live alone, %	59.3	44.4
Living with caregiver, %	33.0	44.4
Living with non-caregiver, %	7.7	11.1
Care-giving support		
No caregiver, %	14.3	22.2
Only live-in caregiver, %	22.0	33.3
Only out-of-home caregiver, %	52.7	33.3
Both in- and out-of-home caregiver, %	11.0	11.1

* $P < 0.05$, ** $P < 0.01$.

depression [10]. Gender differences in depression after widowhood have also been reported [11]. Since women adapt more successfully than men, men who remain alone after losing their partners have a higher risk of developing symptoms of chronic depression.

In our study, despite the level of their disabilities, the prevalence of depressive symptoms among elderly men was low (10.5%). A previous study showed that the prevalence of depression in nursing home residents was very high [7]. Instead of being accommodated in nursing homes, living at home for as long as possible with home care services would allow frail elderly men to maintain their self-esteem and internal locus of control, loss of which might be associated with depression [12].

Depression and cognitive impairment are two of the most frequently observed medical problems in elderly people and often manifest as co-morbid conditions [13]. Approximately 30–40% of those with dementia will experience significant depressive symptoms sometime during the course of the disease [14]. Our study showed that 14.0% of cognitively impaired men (28 out of 200) had depressive symptoms. This seems low when compared with other studies. However, defining depression in demented individuals is a challenge for most health care providers [13]. Patients with dementia are unlikely to be able to express their distress when they feel depressed, and often present with somatic symptoms that are less obviously related to depression [15].

Table 2 Association of independent variables with depressive symptoms from multiple logistic regression analysis

Dependent variable Frequency of dependent variable	Depressive symptoms (21/200) OR (95% CI), *P*
Personal care services	
Duration of services	0.86 (0.75, 0.97)*, *P* = 0.018
Functional status	
Sensory impairment	
Visual impairment	1.14 (0.38, 3.49), *P* = 0.82
Hearing impairment	3.67 (1.18, 11.84)*, *P* = 0.030
Muscular impairment	
Upper extremities impairment	2.61 (0.86, 7.65), *P* = 0.082
Bladder incontinence	1.79 (0.63, 5.11), *P* = 0.28

OR, odds ratio; 95% CI, 95% confidence interval.
* $P < 0.05$.

Untreated depression in dementia can lead to negative consequences, such as a high rate of persistence and increased cognitive impairment, physical disability, social isolation, substance abuse, and suicide [16]. It is important that proper mental health check-ups are provided for cognitively impaired clients.

The high prevalence of hearing impairment among elderly men in our study (46.7%) was consistent with previous studies, whose prevalence rates ranged from 21–72% [17–19]. Hearing impairment leads to withdrawal from social activities and isolation. Previous studies have suggested that hearing impairment in elderly people has a significant correlation with depression [20–24]. Our study was consistent with these findings. People with hearing impairment were 3.67 times more likely to have depressive symptoms than people without a hearing impairment ($P = 0.03$). Hearing impairment needs to be stressed as an indicator of social isolation and the presence of depressive symptoms. Regular audiological check-ups to detect occult hearing impairment, and to provide mental health screening for people with hearing loss, need to be considered.

Depression and ADL disability contributed to their mutual risk [25,26]. ADL disability is a chronic stress producer because, by its very nature, it involves ongoing challenges to the accomplishment of daily tasks [27]. In our study, the number of ADL disabilities was not associated with depressive symptoms. The high prevalence of ADL disability in those making use of personal care services might be too great to allow the detection of any differences in ADL disability between people with and without depressive symptoms.

Epidemiological studies have been consistent in finding an inverse relationship between age and the prevalence of late-life depression [28]. In our study, age did not reach statistical significance in the relationship with depressive symptoms.

Social support is a protective factor for depression among the elderly [29]. Our study did not find any significant associations in the relationship between depressive symptoms and caregiver support.

For every additional year of personal care service use past that of the mean duration, elderly male clients were 14% less likely to be depressed ($P = 0.018$, 95% CI = 0.75–0.97). This suggests that personal care services programs can mitigate the development of depression by keeping clients in their own homes, where they prefer to be the most, for as long as possible.

The main limitation of this study was the potential unreliability of the information on depressive symptoms reported in the M11Q. Primary care physicians complete the M11Q based on their observations, reports from the visiting nurse or from the clients themselves. Delegating responsibility for completing the M11Q to physicians who are not directly involved with the day-to day care of the clients may result in M11Q data that do not reflect the real status of the clients. However, since we employed four indicators of depressive symptoms, this limitation would not account for significant relationships between duration of

services, hearing impairment and depressive symptoms.

Untreated depression in elderly persons negatively influences somatic impairment, adaptation to medical illness, and quality of life, and is associated with increased morbidity and mortality, including suicide [5].

In order to improve the quality of personal care services, it is vital to develop interventions for screening and assessing depressive symptoms among elderly clients who are at risk, and to provide access to specialist mental health services. Intervention focused on elderly men with hearing impairment may be cost-effective, since they are at a high risk for the development of depressive symptoms in later life. We would stress that among various indicators in the administrative data, hearing impairment is important as an indicator of social isolation and the presence of depressive symptoms.

It is also important to introduce personal care services to frail elderly men as soon as they need help, as men tend to be unwilling to get any support because of their masculinity and unfamiliarity with accepting support [30]. Personal care services can improve the circumstances in which they can compensate for their disabilities.

References

[1] Lebanc AL, Tonner CM, Harrington C. State Medicaid programs offering personal care services. Health Care Financ Rev 2001;22:155–73.

[2] Weiner JM, Tilly J, Alecxih LMB. Home and community-based services in seven states. Health Care Financ Rev 2002;23:89–114.

[3] Steven MA, Simone B, Brassard A, Stern Y, Mayeux R. Medicaid home care services and survival in New York City. Gerontologist 2005;45(5):609–16.

[4] Lebowitz BD. Depression and treatment of depression in late life: an overview of the NIH consensus statement. Am J Geriatr Psychiatry 1996;4(Suppl 1):53–6.

[5] Ciechanowski P, Wagner E, Schmaling K, Schwarts S, Williams B, Diehr P, et al. Community-integrated home-based depression treatment in older adults. JAMA 2004; 291(13):1569–77.

[6] Anon, Diagnostic and Statistical Manual of Mental Disorders. Fourth Edition. Washington, DC: American Psychiatric Association; 2004.

[7] Kurlowicz LH, Evans LK, Strumpf NE, Maislin G. A psychometric evaluation of the Cornell Scale for Depression Dementia in a frail, nursing home population. Am J Geriatr Psychiatry 2002;10(5):600–8.

[8] Loughlin A. Depression and social report. J Gerontol Nurs 2004;30(5):11–5.

[9] Piccinelli M, Wilkinson G. Gender differences in depression: critical view. Br J Psychiatry 2000;177:486–92.

[10] Lavretsky H, Kurbranyan K, Ballmaier M, Mintz J, Toga A, Kumar A. Sex differences in brain structure in geriatric depression. Am J Geriatr Psychiatry 2004;12(6):653–7.

[11] van Grootheest DS, Beekaman AT, Broese van Groenou MI, Deeg DJ. Sex differences in depression after widowhood. Do men suffer more? Soc Psychiatry Psychiatr Epidemiol 1999;34(7):391–8.

[12] Bharucha AJ, Dew MA, Miller MD, Borson S, Reynolds 3rd C. Psychotherapy in long-term care: a review. J Am Med Dir Assoc 2006;7(9):568–80.

[13] Leplaire J, Buntinx G. The link between depression and dementia in the elderly. Clin Geriatrics 1999;15:82–7.

[14] Hargrave R, Reed B, Mungas D. Depressive syndrome and functional disorder in dementia. J Geriatr Psychiatry Neurol 2000;13:72–7.

[15] Maynard CK. Differentiate depression from dementia. Nurse Pract 2003;28(3):18–27.

[16] McGrew KB. Mental health services. In Ekerdt DJ, editor-in-chief. Encyclopedia of Aging. New York: Macmillan Reference Books, 2002:923–25.

[17] Morre AA, Siu AL. Screening for common problems in ambulatory elderly: clinical confirmation of a screening instrument. Am J Med 1996;100:438–43.

[18] Feller BA. Prevalence of selected impairments: United States-1977. Vital Health Stat 10 1981;10(134):1–70.

[19] Gates GA, Cooper JC, Kannel WB, Miller NJ. Hearing in the elderly: Framingham cohort 1983–1985. Ear Hear 1990;11:247–56.

[20] Cacciatore F, Napoli C, Abete P, Marciano E, Triassi M, Rengo F. Quality of life determinants and hearing function in an elderly population: Osservatorio Geriatrico Campano Study Group. Gerontology 1999; 45:323–8.

[21] Naramura H, Nakanishi N, Tatara K, Ishikawa M, Shiraishi H, Yamamoto A. Physical and mental correlates of hearing impairment in the elderly in Japan. Audiology 1999;38:24–9.

[22] Uhlmann RF, Larson EB, Rees TS, Koepsell TD, Duckert LG. Relationship of hearing impairment to dementia and cognitive dysfunction in older adults. JAMA 1989; 261:1916–9.

[23] Tambs K. Moderate effects of hearing loss on mental health and subjective well-being: results from the nord-Trondelag hearing loss study. Psychosom Med 2004;66(5):776–82.

[24] Strawbridge WJ, Wallhagen MI, Shema SJ, Kaplan GA. Negative consequences of hearing impairment in old age: a longitudinal analysis. Gerontologist 2000;40(3):320–6.

[25] Bruce ML. The association between depression and disability. Am J Geriatr Psychiatry 1999;7:8–11.

[26] Bruce ML. Depression and disability in late life: direction for future research. Am J Psychiatry 2001;9(2):102–12.

[27] Turner R, Noh S. Physical disability and depression: a longitudinal analysis. J Health Soc Behav 1998;29:23–37.

[28] McAvay GJ, Bruce ML, Raue PJ, Brown EL. Depression in elderly homecare patients: patient versus informant reports. Psychol Med 2004;34:1507–17.

[29] Burnette D, Muri A. Determinants of self-reported depressive symptoms by frail elderly persons living alone. J Gerontol Social Work 1994;22:1–19.

[30] Kosberg JI, Mangum WP. The invisibility of older men in gerontology. Gerontol Geriatr Educ 2002;22(4):27–42.

international journal of andrology ISSN 0105-6263

ORIGINAL ARTICLE

Testosterone decreased urinary-frequency in nNOS-deficient mice

Satoru Muto, Mitsuko Yasuda, Yutaka Kamiyama, Hisamitsu Ide and Shigeo Horie

Department of Urology, Teikyo University, Itabashi-Ku, Tokyo, Japan

Keywords:
bladder overactivity, neuronal nitric oxide synthase, neuronal nitric oxide synthase null mutant mice, testosterone replacement therapy, urinary frequency

Correspondence:
Shigeo Horie, MD, Department of Urology, Teikyo University, 2-11-1 Kaga, Itabashi-ku, Tokyo 173-8605, Japan.
E-mail: shorie@med.teikyo-u.ac.jp

Received 13 December 2006; revised 30 January 2007; accepted 5 February 2007

doi:10.1111/j.1365-2605.2007.00763.x

Summary

To observe the effect of testosterone on the frequency of urination in mice lacking neuronal nitric oxide synthase ($nNOS^{-/-}$), we compared the urination patterns between unanaesthetized male wild-type ($n = 27$) and $nNOS^{-/-}$ mice ($n = 50$) with or without testosterone treatment. Compared with wild-type mice, $nNOS^{-/-}$ mice showed a greater frequency of urination during a 24-h observation period (3.0 vs. 5.4 times/day, $p < 0.0001$) without any significant difference in the total voided volume or the functional voiding capacity. While testosterone treatment did not affect the urination patterns in wild-type, it decreased the daytime frequency of urination (5.4 vs. 3.7 times, $p = 0.0198$) and the nighttime urination (4.4 vs. 2.9 times, $p = 0.039$) in $nNOS^{-/-}$ mice. The $nNOS^{-/-}$ mice can be a useful animal model for urinary frequency. Testosterone improved the functional abnormalities in the voiding of $nNOS^{-/-}$ mice.

Introduction

The relaxation of bladder outlet regions on voiding and the maintenance of low pressure during urinary storage are prerequisite conditions for normal micturition. An accumulating body of evidence indicates that nitric oxide (NO) is an important physiological inhibitory neurotransmitter that mediates relaxation in the smooth muscle component (Andersson *et al.*, 1992; Thornbury *et al.*, 1992; Persson & Andersson, 1994). Nitric oxide is produced as a result of the conversion of the substrate L-arginine to L-citrulline by three isoforms of the enzyme NO synthase (NOS). The mechanism underlying NO-induced smooth muscle relaxation was found to be calcium-dependent, and cyclic guanosine monophosphate (cGMP) was identified as the second messenger. The individual NOS isoforms (eNOS, endothelial nitric oxide synthase; nNOS, neuronal nitric oxide synthase and iNOS, inducible nitric oxide synthase), have a unique subcellular location, structure, kinetics, regulation and function. There is increasing evidence that alterations in the NO–cGMP pathway play an important role in the development of lower urinary tract syndrome (LUTS) (Andersson *et al.*, 2002; Mamas *et al.*, 2003; Chertin *et al.*, 2004; Hedlund, 2005). Neuronally released NO has been suggested to be involved in the relaxation of the urethral smooth muscle during micturition (Buga *et al.*, 1989; Andersson & Persson, 1995; Burnett, 1995). By inhibiting the production of NO, both bladder hyperactivity and a decreased bladder capacity have been demonstrated (Persson *et al.*, 1992).

Indeed a targeted disruption of the nNOS gene has been demonstrated to result in voiding abnormalities (Burnett *et al.*, 1997). In $nNOS^{-/-}$ mice, urinary bladders develop hypertrophy because of deficient outflow relaxation. The urinary bladder and urethra do not relax in response to electrical field stimulation or L-arginine, the amino-acid substrate for NO. The $nNOS^{-/-}$ mice have urinary frequency and a decreased threshold of afferent firing of the bladder detrusor, thus indicating that nNOS is responsible for the relaxation of the bladder outlet regions on voiding and the maintenance of low pressure in urinary storage. These features observed in the abnormal urination of $nNOS^{-/-}$ mice are thus considered to be a plausible model for human overactive bladder.

Recently, several studies have shown testosterone (T) to induce the relaxation of smooth muscle cells by modulating both the nNOS activity and cGMP level. Androgens play a pivotal role in the erectile function by

regulating both cGMP formation by NOS and degradation by phosphodiesterase 5 (PDE5) (Morelli *et al.*, 2005; Vignozzi *et al.*, 2005). In addition, testosterone has direct vasoactive properties. Testosterone has been shown to cause a dose dependant effect on the relaxation of vascular smooth muscles (Webb *et al.*, 1990; English *et al.*, 2001). It is caused either by a direct effect on the vascular smooth muscle, or by an effect on potassium channel (Deenadayalu *et al.*, 2001; English *et al.*, 2002). These lines of evidence prompted us to investigate the role of testosterone in the relaxation of bladder smooth muscle. To evade the effect of nNOS in the relaxation of bladder, $nNOS^{-/-}$ mice was examined to see the role of T. The purpose of the current study was to examine the effect of testosterone on the abnormal voiding of $nNOS^{-/-}$ mice.

Materials and methods

Animals

Experiments were performed in nNOS null mutant mice ($nNOS^{-/-}$) generated by Huang *et al.* (1993) and their wild-type littermates. All wild-type littermates ($n = 27$) and homozygous $nNOS^{-/-}$ males ($n = 50$) of C57Bl/6 strains with targeted disruption of exon2 of the nNOS gene, used in this study were derived from a heterozygous breeding pair. Both groups were housed and studied under identical conditions. At weaning, the animals were ear-tagged. Genomic DNA was extracted from the tails after digestion with proteinase K and E, and purification of DNA with ethanol. The genotype of each DNA sample was then determined by testing for the presence of wild-type or modified nNOS sequences by use of PCR. Animals were maintained on standard rodent chow and tap water at 23 ± 1 °C with a 12/12-h light-dark cycle (lights on at 6:00 AM). The mice always had free access to food and tap water. All care and handling of the animals were carried out in accordance with institutional guidelines.

Voiding behaviour

Male $nNOS^{-/-}$ and wild-type littermates aged 8–13 months and weighing between 30 and 40 gm were used in this study. Voiding studies were carried out after a 3-day period of acclimatization to the laboratory. Individual mice were placed in a mouse micturition cage. The urine collection funnel and faecal separation screen were placed on the bottom of the cage. Each scale was monitored using a remote computer running an application that permits recording information sent by the scale to a resolution of 1 sec. The voiding volume is expressed as weight with a resolution of 10 mg. When assuming a urine specific gravity of approximately, 1.1 mg urine has a volume of 1 mL.

This assumption was reasonable because animals with polydipsia tend to produce extremely dilute urine. The total amount of urine voided in 1 day was accumulated into a container. Voiding was studied continuously for a 10-day period.

Testosterone administration

After stable baseline voiding patterns had been established, 3.6 mg/g body weight testosterone enanthate (Teikoku Hormone Mfg, Tokyo, Japan) diluted in sesame oil or other vehicles were singly administered intraperitoneally to male wild-type littermates and $nNOS^{-/-}$. This dose was selected based on previous studies that examined the effect of androgen on the gene expression in the prostate (Mirosevich *et al.*, 1999, 2001). The voiding pattern of the treated mice was examined 1-week later. We examined the urinary frequency, functional bladder capacity and the urinary volume.

Statistics

The results are generally reported as the mean ± SD. Student's unpaired two-tailed t test was used compared with the micturition parameters between the control and obstructed groups, as well as between the wild-type littermates and $nNOS^{-/-}$. One-way ANOVA was used to analyse to compare the differences of the parameters among four groups (wild-type with or without testosterone and $nNOS^{-/-}$ with or without T). A probability level of <0.05 was considered to be significant.

Results

The micturitional characteristics of wild-type and $nNOS^{-/-}$ mice

The amount of urine output per day (0.84 ± 0.40 mL vs. 1.09 ± 0.55 mL, $p = 0.282$) and the functional bladder capacity (defined as the voided volume per void) (0.28 ± 0.17 mL vs. 0.21 ± 0.12 mL, $p = 0.061$) did not differ substantially between the wild-type and $nNOS^{-/-}$ mice. Within comparison to the wild-type mice, the $nNOS^{-/-}$ mice showed a greater frequency of urination during the 24-h observation period (3.00 ± 1.00 times vs. 5.40 ± 0.97 times, $p < 0.0001$) and also during the nocturnal period (2.50 ± 0.85 times vs. 4.40 ± 1.27 times, $p = 0.001$) (Table 1).

However, no significant differences were seen in the frequency of daytime voiding between the wild type and $nNOS^{-/-}$ mice (0.50 ± 0.71 times vs. 0.60 ± 0.70 times, $p = 0.750$).

Table 1 The number of voids in wild-type and nNOS$^{-/-}$ mice

	WT (n = 27)	KO (n = 50)	p-value
Capacity			
Total micturition volume (mL/24 h)	0.84 ± 0.40	1.09 ± 0.55	0.282
Functional capacity (mL/void)	0.28 ± 0.17	0.21 ± 0.12	0.061
	WT (n = 10)	KO (n = 10)	
frequency			
No. of voids/24 h	3.00 ± 1.00	5.40 ± 0.97	<0.0001
No. of daytime voids	0.50 ± 0.71	0.60 ± 0.70	0.750
No. of nightime voids	2.50 ± 0.85	4.40 ± 1.27	0.001

WT, wild-type; KO, neuronal nitric oxide synthase (nNOS$^{-/-}$).

Effects of testosterone on the urinary frequency of nNOS$^{-/-}$ and the wild-type mice

Testosterone treatment did not affect either the amount of urine output per day (wild-type; 0.84 ± 0.40 mL vs. 0.64 ± 0.57 mL, p = 0.420, nNOS$^{-/-}$; 1.09 ± 0.55 mL vs. 1.01 ± 0.59 mL, p = 0.782) or the functional bladder capacity (wild-type; 0.28 ± 0.17 mL vs. 0.24 ± 0.13 mL, p = 0.331, nNOS$^{-/-}$; 0.21 ± 0.12 mL vs. 0.27 ± 0.10 mL, p = 0.057) in the wild-type and nNOS$^{-/-}$ mice. Regarding the frequency of daytime voiding, there were no significant differences before and after testosterone administration in the wild-type and nNOS$^{-/-}$ mice (wild-type; 0.50 ± 0.71 times vs. 1.33 ± 1.37 times, p = 0.127, nNOS$^{-/-}$; 0.60 ± 0.70 times vs. 0.86 ± 0.69 times, p = 0.465). However, in the nNOS$^{-/-}$ mice, testosterone administration significantly decreased the frequency of urination during both the 24-h observation period (5.40 ± 0.97 times vs. 3.71 ± 1.70 times, p = 0.020) and the nocturnal period (4.40 ± 1.27 times vs. 2.86 ± 1.86 times, p = 0.039). By one-way ANOVA, there were statistical differences in both the 24-h observation period (p =0.018) and the nocturnal period (p < 0.001) among four groups (wild-type with or without testosterone nNOS$^{-/-}$ mice with or without T) (Table 2).

Discussion with conclusions

In the present study, we confirmed the previous study that nNOS$^{-/-}$ mice had urinary frequency with a decreased functional urinary bladder capacity. Thus nNOS$^{-/-}$ mice can be a useful animal model for the exploration of the treatment of LUTS. Several lines of evidence may allow the speculation for the underlying mechanisms of the effect of the testosterone treatment on the voiding abnormalities of nNOS$^{-/-}$ mice.

First, testosterone has been shown to cause a dose-dependant effect on the relaxation of vascular smooth muscles (Webb *et al.*, 1990; English *et al.*, 2001). However, it remained unknown whether testosterone relaxes smooth muscle cell in a tonic manner. Secondly, there is evidence that androgens can regulate the expression of NOS enzymes in the corporeal tissue (Chamness *et al.*, 1995; Park *et al.*, 1999). As a result, in nNOS$^{-/-}$ mice, testosterone might possibly augment the expression of eNOS to compensate for the loss of nNOS. A previous study demonstrated that androgens maintain the erectile response by the pathways that are independent of NO but involve the synthesis of cGMP (Reilly *et al.*, 1997). Those hypotheses warrant further studies. The association of the late-onset hypogonadism and urinary frequency has been reported in literature. The findings of this study may indicate that testosterone potentially has a therapeutic effect on an overactive bladder by decreasing the nNOS expression in ageing males. The nNOS$^{-/-}$ mice showed an increased urinary frequency. Testosterone treatment significantly improved the urinary frequency for nNOS$^{-/-}$ mice. These findings may indicate that testosterone can improve bladder overactivity because of the loss of nNOS. Androgen replacement may therefore be a potentially useful and novel pharmacological target for patients with a decreased level of NO thus leading to urinary frequency.

Table 2 The voiding function in wild-type and nNOS$^{-/-}$ mice before and after testosterone administration

	WT (n = 27)	WT + T (n = 19)	p-value	KO (n = 50)	KO + T (n = 26)	p-value
Capacity						
Total micturition volume (mL/24 h)	0.84 ± 0.40	0.64 ± 0.57	0.420	1.09 ± 0.55	1.01 ± 0.59	0.782
Functional capacity (mL/void)	0.28 ± 0.17	0.24 ± 0.13	0.331	0.21 ± 0.12	0.27 ± 0.10	0.057
	WT (n = 10)	WT + T (n = 7)		KO (n = 10)	KO + T (n = 7)	
Frequency						
No. of voids/24 h	3.00 ± 1.00	2.71 ± 2.22	0.734	5.40 ± 0.97	3.71 ± 1.70	0.020
No. of daytime voids	0.50 ± 0.71	1.33 ± 1.37	0.127	0.60 ± 0.70	0.86 ± 0.69	0.465
No. of nightime voids	2.50 ± 0.85	1.33 ± 1.21	0.059	4.40 ± 1.27	2.86 ± 1.86	0.039

WT, wild-type; WT + T, wild-type after testosterone administration; KO, neuronal nitric oxide synthase (nNOS$^{-/-}$); KO + T, nNOS$^{-/-}$ after testosterone administration.

References

Andersson, K. E. & Persson, K. (1995) Nitric oxide synthase and the lower urinary tract: possible implications for physiology and pathophysiology. *Scandinavian Journal of Urology and Nephrology* 175, 43–53.

Andersson, K. E., Garcia Pascual, A., Persson, K., Forman, A. & Tottrup, A. (1992) Electrically-induced, nerve-mediated relaxation of rabbit urethra involves nitric oxide. *Journal of Urology* 147, 253–259.

Andersson, K. E., Chapple, C. R. & Hofner, K. (2002) Future drugs for the treatment of benign prostatic hyperplasia. *World Journal of Urology* 19, 436–442.

Buga, G. M., Gold, M. E., Wood, K. S., Chaudhuri, G. & Ignarro, L. J. (1989) Endothelium-derived nitric oxide relaxes non-vascular smooth muscle. *European Journal Pharmacology* 161, 61–72.

Burnett, A. L. (1995) Nitric oxide control of lower genitourinary tract functions: s review. *Urology* 45, 1071–1083.

Burnett, A. L., Calvin, D. C., Chamness, S. L., Liu, J. X., Nelson, R. J., Klein, S. L., Dawson, V. L., Dawson, T. M. & Snyder, S. H. (1997) Urinary bladder-urethral sphincter dysfunction in mice with targeted disruption of nNOS models idiopathic voiding disorders in humans. *Nature Medicine* 3, 571–574.

Chamness, S. L., Ricker, D. D., Crone, J. K., Dembeck, C. L., Maguire, M. P., Burnett, A. L. & Chang, T. S. (1995) The effect of androgen on NOS in the male reproductive tract of the rat. *Fertility and Sterility* 63, 1101–1107.

Chertin, B., Rolle, U., Solari, V., Cascio, S. & Puri, P. (2004) The role of nitric oxide in bladder urothelial injury after bladder outlet obstruction. *BJU International* 94, 392–399.

Deenadayalu, V. P., White, R. E., Stallone, J. N., Gao, X. & Garcia, A. J. (2001) Testosterone relaxes coronary arteries by opening the large-conductance, calcium-activated potassium channel. *American Journal of Physiology Heart and Circulatory Physiology* 281, H1720–1727.

English, K. M., Jones, R. D., Jones, T. H., Morice, A. H. & Channer, K. S. (2001) Gender differences in the vasomotor effects of different steroid hormones in rat pulmonary and coronary arteries. *Hormone and Metabolic Research* 33, 645–652.

English, K. M., Jones, R. D., Jones, T. H., Morice, A. H. & Channer, K. S. (2002) Testosterone acts as a coronary vasodilator by a calcium channel antagonist action. *Journal of Endocrinological Investigation* 25, 455–458.

Hedlund, P. (2005) Nitric oxide/cGMP-mediated effects in the outflow region of the lower urinary tract: is there a basis for pharmacological targeting of cGMP? *World Journal of Urology* 23, 362–367.

Huang, P. L., Dawson, T. M., Bredt, D. S., Snyder, S. H. & Fishman, M. C. (1993) Targeted disruption of the neuronal nitric oxide synthase gene. *Cell* 75, 1273–1286.

Mamas, M. A., Reynard, J. M. & Brading, A. F. (2003) Nitric oxide and the lower urinary tract: current concepts, future prospects. *Urology* 61, 1079–1085.

Mirosevich, J., Bentel, J. M., Zeps, N., Redmond, S. L., D'Antuono, M. F. & Dawkins, H. J. (1999) Androgen receptor expression of proliferating basal and luminal cells in adult murine ventral prostate. *The Journal of Endocrinology* 162, 341–350.

Mirosevich, J., Bentel, J. M. & Dawkins, J. S. (2001) Regulation of caltrin mRNA expression by androgens in the murine prostate. *Journal of Andrology* 22, 449–457.

Morelli, A., Filippi, S., Zhang X. H., Luconi, M., Vignozzi, L., Mancina, R. & Maggi, M. (2005) Hormonal regulation of peripheral regulatory mechanisms in erection. *International Journal of Andrology* 28, 23–27.

Park, K. H., Kim, S. W., Kim, K. D. & Paick, J. S. (1999) Effects of androgens on the expressions of nitric oxide synthase mRNAs in rat corpus cavernosum. *BJU International* 83, 327–333.

Persson, K. & Andersson, K. E. (1994) Non-adrenergic, non-cholinergic relaxation and levels of cyclic nucleotides in rabbit lower urinary tract. *European Journal of Pharmacology* 268, 159–167.

Persson, K., Igawa, Y., Mattiasson, A. & Andersson, K. E. (1992) Effects of inhibition of the L-arginine/nitric oxide pathway in urinary tract in vivo and in vitro. *British Journal of Pharmacology* 107, 178–184.

Reilly, C. M., Lewis, R. W., Stopper, V. S. & Mills, T. M. (1997) Androgenic maintenance of the rat erectile response via a non-nitric oxide-dependent pathway. *Journal of Andrology* 18, 588–594.

Thornbury, K. D., Hollywood, M. A. & McHale, N. G. (1992) Mediation by nitric oxide of neurogenic relaxation of the urinary bladder neck muscle in sheep. *The Journal of Physiology* 451, 133–144.

Vignozzi, L., Corona, G., Petrone, L., Filippi, S., Morelli, A. M., Forti, G. & Maqqi, M. (2005) Testosterone and sexual activity. *Journal of Endocrinological Investigation* 28, 39–44.

Webb, C. M., McNeill, J. G., Hayward, C. S., de Zeigler, D. & Collins, P. (1990) Effects of testosterone on coronary vasomotor regulation in men with coronary heart disease. *Circulation* 100, 1690–1696.

Atrazine-Induced Aromatase Expression Is SF-1 Dependent: Implications for Endocrine Disruption in Wildlife and Reproductive Cancers in Humans

WuQiang Fan,[1] Toshihiko Yanase,[1] Hidetaka Morinaga,[1] Shigeki Gondo,[1] Taijiro Okabe,[1] Masatoshi Nomura,[1] Tomoko Komatsu,[2] Ken-Ichirou Morohashi,[2] Tyrone B. Hayes,[3] Ryoichi Takayanagi,[1] and Hajime Nawata[4]

[1]Department of Medicine and Bioregulatory Science, Graduate School of Medical Science, Kyushu University, Fukuoka, Japan; [2]Department of Developmental Biology, National Institute for Basic Biology, Okazaki, Japan; [3]Laboratory for Integrative Studies in Amphibian Biology, Group in Endocrinology, Museum of Vertebrate Zoology, Energy and Resources Group, and Department of Integrative Biology, University of California, Berkeley, California, USA; [4]Graduate School of Medical Science, Kyushu University, Fukuoka, Japan

BACKGROUND: Atrazine is a potent endocrine disruptor that increases aromatase expression in some human cancer cell lines. The mechanism involves the inhibition of phosphodiesterase and subsequent elevation of cAMP.

METHODS: We compared steroidogenic factor 1 (SF-1) expression in atrazine responsive and nonresponsive cell lines and transfected SF-1 into nonresponsive cell lines to assess SF-1's role in atrazine-induced aromatase. We used a luciferase reporter driven by the SF-1–dependent aromatase promoter (ArPII) to examine activation of this promoter by atrazine and the related simazine. We mutated the SF-1 binding site to confirm the role of SF-1. We also examined effects of 55 other chemicals. Finally, we examined the ability of atrazine and simazine to bind to SF-1 and enhance SF-1 binding to ArPII.

RESULTS: Atrazine-responsive adrenal carcinoma cells (H295R) expressed 54 times more SF-1 than nonresponsive ovarian granulosa KGN cells. Exogenous SF-1 conveyed atrazine-responsiveness to otherwise nonresponsive KGN and NIH/3T3 cells. Atrazine induced binding of SF-1 to chromatin and mutation of the SF-1 binding site in ArPII eliminated SF-1 binding and atrazine-responsiveness in H295R cells. Out of 55 chemicals examined, only atrazine, simazine, and benzopyrene induced luciferase via ArPII. Atrazine bound directly to SF-1, showing that atrazine is a ligand for this "orphan" receptor.

CONCLUSION: The current findings are consistent with atrazine's endocrine-disrupting effects in fish, amphibians, and reptiles; the induction of mammary and prostate cancer in laboratory rodents; and correlations between atrazine and similar reproductive cancers in humans. This study highlights the importance of atrazine as a risk factor in endocrine disruption in wildlife and reproductive cancers in laboratory rodents and humans.

KEY WORDS: aromatase, atrazine, breast cancer, cAMP, *CYP19*, endocrine disruptor, hermaphroditism, prostate cancer, SF-1. *Environ Health Perspect* 115:720–727 (2007). doi:10.1289/ehp.9758 available via *http://dx.doi.org/* [Online 5 February 2007]

Atrazine, a triazine herbicide used primarily in corn production (Frank and Sirons 1979), is the most common pesticide contaminant of groundwater and surface water (Fenelon and Moore 1998; Hennion M, Pichon V, Legeay P, Cohen M, unpublished data; Kolpin et al. 1998; Lode et al. 1995; Miller et al. 2000; Müller et al. 1997; Solomon et al. 1996; Thurman and Cromwell 2000). In addition to its high use, ubiquitous contamination of aquatic environments, persistence, and mobility, atrazine is a concern because it is a potent endocrine disruptor in wildlife and laboratory rodents.

A U.S. Environmental Protection Agency (EPA) laboratory first concluded that atrazine was an endocrine disruptor in the year 2000:

> Atrazine tested positive in the pubertal male screen that the EDSTAC [U.S. EPA Endocrine Disruptor Screening and Testing Advisory Committee] is considering as an optional screen for endocrine disruptors. (Stoker et al. 1999)

Among other endocrine-disrupting effects (Babic-Gojmerac et al. 1989; Cooper et al. 1999, 2000; Cummings et al. 2000; Friedmann 2002; Kniewald et al. 1979, 1995; Narotsky et al. 2001; Shafer et al. 1999; Šimic et al. 1991; Stoker et al. 1999, 2000), atrazine disrupts androgen- and estrogen-mediated processes. Atrazine has a low affinity for androgen and estrogen receptors (Roberge et al. 2004; Tennant et al. 1994) and, thus, is not a receptor agonist or antagonist. Atrazine reduces androgen synthesis and action via several mechanisms (Babic-Gojmerac et al. 1989; Kniewald et al. 1979, 1980, 1995; Šimic et al. 1991) and it increases estrogen production (Crain et al. 1997; Heneweer et al. 2004; Keller and McClellan-Green 2004; Sanderson et al. 2000, 2001, 2002; Spano et al. 2004).

Atrazine increases aromatase levels by binding to and inhibiting phosphodiesterase (Roberge et al. 2004; Sanderson et al. 2000, 2001), resulting in elevated cAMP in some human cancer cell lines. Elevated cAMP results in increased transcription of the aromatase gene *CYP19* [cytochrome P450, family 19, subfamily A, polypeptide 1 (CYP19A1); UniGene Hs.654384 (UniGene 2007) or GenBank NM_000103 (GenBank 2007)], increased aromatase activity, and, ultimately, increased estrogen production. The molecular mechanism is not completely understood, however, and effects vary between cell types (Morinaga et al. 2004). In this article we address the role of the important transcription factor, steroidogenic factor 1 (SF-1), in atrazine-induced aromatase expression.

Materials and Methods

Experiments. Experiment 1: SF-1 levels in atrazine-responsive and -nonresponsive cells. To test the hypothesis that SF-1 is required for atrazine-induced aromatase expression, we examined SF-1 levels in atrazine-responsive H295R adrenocortical carcinoma cells and nonresponsive KGN granulosa cells. Endogenous SF-1 mRNA was analyzed by real-time polymerase chain reaction (PCR) with the relative copies of SF-1 to β-actin in KGN cells set to 1. The relative copies of SF-1 to β-actin in H295R cells were calculated accordingly. SF-1 protein levels were confirmed by Western blot analysis.

Experiment 2: Induction of luciferase activity by atrazine and simazine via aromatase promoter II in H295R cells. We transfected H295R and NIH/3T3 cells with a 4.0 kb aromatase promoter II (ArPII) luciferase reporter (pGL3-ArPII4.0) with or without cotransfection with human SF-1 (pcDNA3.1-hSF-1). This experiment was designed to determine whether SF-1 would increase the

Address correspondence to T.B. Hayes, Department of Integrative Biology, University of California, Berkeley, CA 94720-3104 USA. Telephone: (510) 643-1054. Fax: (510) 643-6264. E-mail: tyrone@berkeley.edu

We thank E.R. Simpson for the generous gift of the luciferase reporter plasmids of ArPII-516 and ArPII-516-SF1-M; and K.-I. Morohashi for the anti-SF-1 antibody and the baculo-virus vector for mouse SF-1.

The study was supported by a grant-in-aid for "Mechanisms of Sex Differentiation" and a grant for the 21st Century COE program from the Ministry of Education, Culture, Sports, Science and Technology of Japan. No U.S. federal funds were used in these studies. T.B.H. was funded by the University of California, Berkeley.

The authors declare they have no competing financial interests.

Received 22 September 2006; accepted 5 February 2007.

ability of atrazine to induce gene expression via ArPII using a luciferase promoter.

Experiment 3: Other environmental contaminants. We used a luciferase activity assay [NIH/3T3 cells co-transfected with 4.0 kb ArPII reporter (pGL3-ArPII4.0) and human SF-1 (pcDNA3.1-hSF-1)] to screen 55 environmental contaminants. Cells were exposed to the solvent (DMSO) or 10^{-6} mol/L forskolin [protein kinase A (PKA) agonist] with or without each of 55 chemicals at 10^{-5} mol/L (except for 10^{-7} mol/L tributyltin and 10^{-7} mol/L triphenyltin) for 48 hr before the luciferase assay was performed.

Experiment 4: Atrazine induction of aromatase expression and activity in KGN ovarian cells. We used KGN ovarian cells to examine aromatase expression in response to atrazine exposure. SF-1 infection of KGN cells was used to determine whether this transcription factor was sufficient to support atrazine-induced aromatase in this otherwise atrazine nonresponsive cell line.

Experiment 5: Atrazine-enhanced SF-1 binding to ArPII. We conducted a chromatin-immunoprecipitation (ChIP) assay to determine whether atrazine and simazine increased binding of SF-1 to ArPII.

Experiment 6: Binding of atrazine to SF-1. We used surface plasmon resonance (SPR) to examine the ability of atrazine to bind directly to SF-1 as a second mechanism by which atrazine could induce gene expression via ArPII. We used quartz crystal balance techniques to confirm results of the SPR study.

Chemical standards. Chemicals standards for testing in cell lines were obtained from Wako Pure Chemical Co. (Osaka, Japan) and Accu Standard, Inc. (New Haven, CT, USA). We examined the effects of these chemicals, at a concentration of 10^{-5} mol/L (except for 10^{-7} mol/L tributyltin and 10^{-7} mol/L triphenyltin). The chemicals were dissolved in ethanol (except for aldicarb, atrazine, and simazine, which were dissolved in DMSO) at the original concentration of 10^{-2} mol/L. The adenylyl cyclase activator forskolin was purchased from Sigma-Aldrich, Inc. (St. Louis, MO, USA) and was dissolved in DMSO.

Cell lines. The human ovarian granulosa-like tumor cell line (KGN) was established and maintained as previously reported (Nishi et al. 2001). H295R adrenal carcinoma cells (ATCC CRL 2128), NIH/3T3 mouse fibroblasts (ATCC CRL1658), and sf21 insect cells (ATCC CRL1711) were all obtained from the American Type Culture Collection (ATCC; Manassas, VA, USA) and grown under culture conditions prescribed by the ATCC.

Plasmids and constructs. We constructed a luciferase reporter containing 4.0 kb of the 5′-flanking sequence of *ArPII* as previously described (Fan et al. 2005a). A 4-kb human SF-1 promoter luciferase reporter was established previously (Oba et al. 2000). We purchased the Renilla luciferase reporter plasmid pRL-CMV from Promega (Madison, WI). An adenovirus construct expressing bovine SF-1 (adeno-SF-1) and another expressing β-galactosidase (adeno-LacZ) were prepared as described previously (Gondo et al. 2004).

Quantification of mRNA. Total RNA from cells was isolated and reverse-transcribed to cDNA; relative aromatase mRNA copy numbers to β-actin were then analyzed by real-time PCR following the protocol described previously (Fan et al. 2005b). Primers for human aromatase were 5′-ACG CAG GAT TTC CAC AGA AGA G-3′ (forward) and 5′-CTT CTA AGG CTT TGC GCA TGA C-3′ (reverse). Primers for human β-actin were 5′-AAA CTA CCT TCA ACT CCA TC-3′ (forward) and 5′-ATG ATC TTG ATC TTC ATT GT-3′ (reverse). Endogenous human SF-1 mRNA copies in H295R and KGN cells were also determined by the same method. Primers for SF-1 were 5′-CAG CCT GGA TTT GAA GTT CC-3′(forward) and 5′-TTC GAT GAG CAG GTT GTT GC-3′ (reverse).

Western blots. Western blots were conducted using standard techniques. The anti-SF-1 antibody used was provided by K. Morohashi (National Institution for Basic Biology, Okazaki, Japan).

Relative luciferase reporter assay. For the 55 environmental chemical-screening studies, we co-transfected each of three 10-cm^2 dishes containing 70% confluent NIH-3T3 cells with 1.5 μg ArPII reporter (PGL3-ArPII4.0), 1.5 μg pcDNA3.1-hSF-1, and 10 ng pRL-CMV by Effectence transfection reagent (QIAGEN, Miami, FL, USA) following the manufacturer's protocol. Twenty-four hours after transfection, cells in all three dishes were trypsinized, mixed together, and reseeded to 24-well plates (approximately 1.0×10^5 cells/well). DMSO, 10^{-6} mol/L forskolin, or 10^{-5} mol/L test chemicals plus forskolin was added to the cells, and a luciferase assay was performed 48 hr later. The basic technical details for other relative dual-luciferase assays in this study are as follows. On the first day, 0.75×10^5 cells/well in 0.5 mL growth medium were seeded into 24-well plates. On the second day, 0.4 μg PGL3-ArPII, 1.0 ng pRL-CMV, and 0.1 μg pcDNA3.1-hSF-1, or an equal-molar amount of empty vector pcDNA3.1, were transiently co-transfected to each well using the Effectence transfection reagent. On the third day, the culture medium was replaced with fresh medium in the presence of proper chemicals or its solvent DMSO. On the fifth day (48 hr after chemical treatment), the cells were lysed in 100 μL/well passive lysis buffer, and the luciferase assay was performed in accordance with the protocol of the Dual-Luciferase Reporter Assay System (Promega) using a Lumat LB 9507 luminometer (Berthold Technologies, Bad Wildbad, Germany). The firefly luciferase activity produced by PGL3-ArPII in identically treated triplicate samples was normalized for the renilla luciferase activity produced by pRL-CMV. The data shown represent at least three independent experiments.

Aromatase assay. We measured ^3H_2O released upon conversion of [1β-^{3}H] androstenedione to estrone to measure aromatase activity, as described previously (Mu et al. 2000). Briefly, the cells were cultured in a 24-well dish in Dulbecco's modified Eagle's medium/Ham's F-12 with 10% fetal bovine serum in the presence of atrazine, simazine, or DMSO and incubated for 40 hr. The cells were then incubated with [1β-^{3}H] androstenedione for an additional 6 hr. The medium was extracted with chloroform and centrifuged. The aqueous phase was then mixed with 5% charcoal/0.5% dextran and incubated for 30 min. The mixture was subsequently centrifuged, and the supernatant was added to 5 mL scintillation fluid and assayed for radioactivity. The amount of radioactivity in ^3H_2O was standardized from the protein concentration determined using a protein assay kit (Bio-Rad Laboratories, Hercules, CA, USA).

ChIP assay. ChIP assays were performed using the ChIP assay kit from Upstate Biotechnology (Lake Placid, NY, USA) following the protocol provided by the manufacturer, with some modifications. Briefly, H295R cells were seeded in 10-cm^2 dishes and treated with 10^{-5} mol/L atrazine, simazine, or DMSO for 48 hr. Cells were then cross-linked with 1% formaldehyde for 60 min, washed with chilled phosphate-buffered saline (PBS), resuspended in 200 μL SDS lysis buffer, and sonicated six times for 10 sec each at 60% maximum setting of the sonicator (Handy Sonic-UR-20P; TOMY SEIKO Co., Ltd., Tokyo, Japan). Sonicated cell supernatant was diluted 10-fold, and 1% (20 μL) of the total diluted lysate was used for total genomic DNA as input DNA control. The rest (1,980 μL) was then subjected to immunoclearing by 75 μL salmon sperm DNA/protein A agarose–50% slurry for 30 min at 4°C. Immunoprecipitation was performed overnight at 4°C with 3 μg anti-SF-1 antibody (courtesy of K. Morohashi, National Institution for Basic Biology, Okazaki, Japan). For the negative control, we used normal rabbit IgG (Santa Cruz Biotechnology) instead of the antibody. Precipitates were washed sequentially for 5 min each in low-salt, high-salt, and lithium chloride immune complex wash buffers, and finally washed twice with Tris/EDTA buffer. Histone complexes were then eluted from the antibody by freshly prepared elution buffer (1% SDS, 0.1 M $NaHCO_3$). Histone-DNA cross-links (including the input samples) were reversed by 5 M NaCl at 65°C for 4 hr. DNA fragments were extracted with a

PCR purification kit (Qiagen, Valencia, CA). We used 1 μL from a 30-μL DNA extraction for PCR (28 cycles) and primed by sequences as follows: forward, 5′-GGG AAG AAG ATT GCC TAA AC-3′; reverse, 5′-TGT GGA AAT CAA AGG GAC AG-3′; the PCR size was 401 bp. Immunoprecipitated DNA samples were then set to real-time PCR analysis to quantify the relative amount to their corresponding input controls with a LightCycler (Roche Diagnostics GmbH, Mannheim, Germany) according to the manufacturer's instructions. Briefly, 1 μL immunoprecipitated DNA sample (or H_2O as negative control), was placed into a 20-μL reaction volume containing 1 μL of each primer (10 μM) and 2 μL LightCycler-FastStart DNA Master SYBR Green I (Roche), which includes nucleotides, Tag DNA polymerase, and buffer. Input samples were amplified simultaneously as the internal controls. Real-time PCR data for each immunoprecipitated sample were calculated as a ratio to the corresponding input sample. Briefly, threshold values (crossing line) obtained where fluorescent intensity was in the geometric phase, cycle number at the crossing point of an immunoprecipitated sample (Cip), and the corresponding input sample (Cco) were determined via LightCycler software, version 3.5. The relative amount of the immunoprecipitated sample (Aip) to input sample was calculated by the formula $Aip = 2^{(Cco - Cip)}$.

We also performed deletion–mutation assays on the 4.0 kb ArPII to identify the responsible site for atrazine and simazine stimulation. The promoter was cut down using restriction enzymes (*Sna*BI, *Afl*II, or *Eco*RI) to make three other ArPII reporters with lengths of 3.1 kb, 2.0 kb, and 1.0 kb, respectively. Responsiveness was indicated by 10^{-5} mol/L atrazine-induced multiples of relative luciferase activity (RLA) mediated by each promoter. The 516 bp ArPII luciferase reporter (PGL3-PII-516) and the PGL3-PII-516-SF1-M (of which the SF-1 site was mutated from AGGTCA to ATTTCA) were provided courtesy of E.R. Simpson (Monash University, Melbourne, Australia) (Rubin et al. 2002).

Surface plasmon resonance. We used baculovirus to express the Flag containing SF-1 fusion protein in insect sf21 cells. The baculovirus mouse SF-1 expression vector was established as described previously (Komatsu et al. 2004). Sf21 cells were infected with baculovirus, and extracts were prepared 72 hr postinfection. The Flag-SF-1 fusion protein was purified by affinity chromatography with anti-Flag M2 antibody-agarose (Sigma, St. Louis, MO, USA) and eluted with 150 μg/mL 3 × Flag peptide (Sigma). The binding affinity of atrazine to Flag-SF-1 was measured by Surface Plasmon Resonance (SPR) using a Biocore T100 biosensing system (Biocore, Tokyo, Japan) following the standard manufacturer's protocol. The Biocore T100 can investigate interactions involving binding partners with molecular weight as low as 100 Da. Purified Flag-SF-1 protein (11700–14250 resonance units) was immobilized on a Series S Sensor Chip (CM5; Biocore) by using the Amincoupling kit (Biocore). Chemicals [atrazine as the one of interest; 1,2-dihexadecanoyl-*n*-glycero-3-phosphocholine (16PC) as the positive control; benzophenone and *p*-nitrotoluene as negative controls) were dissolved in PBS (pH 7.4) + 5% DMSO at various concentrations. PBS + 5% DMSO was used as the mobile phase medium (running buffer) at a flow rate of 30 μL/min at 25°C. Binding of chemicals dissolved in the running buffer to immobilized Flag-SF-1 was monitored in real time by measuring changes in resonance units. The sensorgrams for the reference channel (non-SF-1–bearing CM5 chip) were subtracted simultaneously from the sensorgrams for sensing channel (SF-1 bearing CM5 chip). All data were automatically analyzed by Biocore T100 evaluation software (version 1.00).

Quartz crystal microbalance. We examined binding of atrazine to SF-1 using a 27-MHz quartz crystal microbalance (QCM; Initium Co., Tokyo, Japan). SF-1 was immobilized onto a QCM electrode according to the manufacturer's protocol. The electrode was soaked in 8 mL PBS buffer (pH 7.4) and monitored continuously for QCM frequency change at 25°C. After the frequency change was stabilized, chemicals of interest were added to the solution and we assessed the time course of frequency change in response to the addition of chemicals.

Statistical analysis. All data are expressed as the mean ± SD and were evaluated by one-way analysis of variance (ANOVA) or two-tailed Student's *t*-test, followed by post hoc comparisons with Fisher's protected least-significant-difference test. $p < 0.05$ was considered statistically significant.

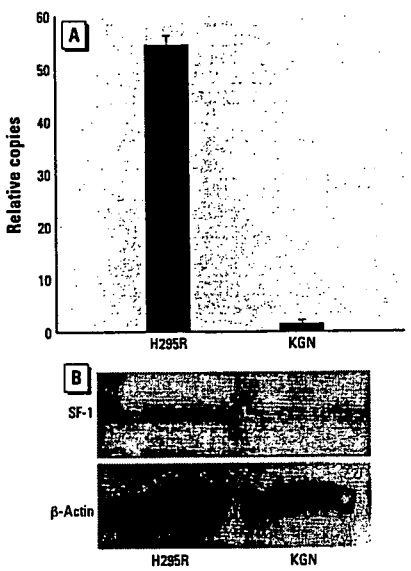

Figure 1. Effects of SF-1 on induction of *CYP19* by 10^{-5} mol/L atrazine. (*A*) SF-1 expression was significantly higher (54-fold; ANOVA, $p < 0.05$) in atrazine-responsive H295R cells compared with atrazine-nonresponsive KGN cells. (*B*) SF-1 protein levels were also higher in H295R cells as determined by Western blot.

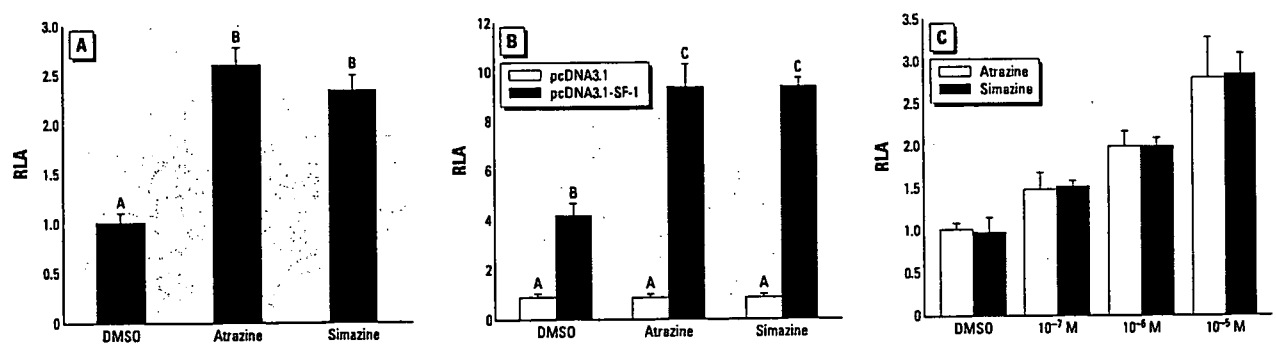

Figure 2. Effects of atrazine and simazine (10^{-5} mol/L each for *A* and *B*; as marked for *C*) of three cell types, measured by RLA. (*A*) Atrazine and simazine stimulated ArPII in H295R cells without exogenous SF-1 supplementation. (*B*) ArPII response to atrazine and simazine in NIH-3T3 cells required coexpression of SF1. (*C*) Atrazine and simazine stimulation of SF-1–mediated ArPII in SF-1–co-transfected NIH-3T3 cells was dose dependent. Both triazines were effective at concentrations as low as 10^{-7} mol/L (ANOVA, $p < 0.05$). Bars show mean ± SD; letters above bars indicate statistical groups (ANOVA, $p < 0.05$).

Results

Experiment 1. Although the nonresponsive KGN granulosa cells expressed SF-1 mRNA, real-time PCR revealed that copy numbers of SF-1 mRNA were 54 times lower in these atrazine nonresponsive cells compared with the atrazine-responsive H295R adrenocortical carcinoma cells (ANOVA, $p < 0.05$; Figure 1A). A concomitant Western-blot analysis revealed markedly higher SF-1 protein levels in atrazine-responsive H295R adrenocortical carcinoma cells compared with the nonresponsive KGN granulosa cells (Figure 1B).

Experiment 2. Atrazine and simazine (a similar triazine herbicide) both induced luciferase activity in H295R adrenocortical carcinoma cells (which express SF-1 endogenously) without co-transfection of SF-1 (ANOVA, $p < 0.05$; Figure 2A). Neither atrazine nor simazine affected ArPII in the absence of SF-1 coexpression in NIH/3T3 fibroblast cells, which lack endogenous SF-1 expression (ANOVA, $p > 0.05$; Figure 2B). Once SF-1 was present (pcDNA3.1-hSF-1–co-transfected cells), however, there was a 4.2-fold elevation in basal activity and increased responsiveness to atrazine and simazine (ANOVA, $p < 0.05$; Figure 2B). Both atrazine and simazine increased SF-1–enhanced ArPII activity 2.25- and 2.26-fold, respectively (ANOVA, $p < 0.05$; Figure 2B) in the pcDNA3.1-hSF-1–transfected NIH/3T3 cells. The 2.2- and 2.3-fold are similar to the chlorotriazine-stimulation of ArPII activity in H295R (SF-1 nontransfected). Thus, the ArPII response to atrazine and simazine is SF-1 dependent. Furthermore, in these SF-1 coexpressing NIH/3T3 cells, the atrazine/simazine stimulation of SF-1–mediated ArPII was dose dependent, with both chemicals effective at concentrations as low as 10^{-7} mol/L (ANOVA, $p < 0.05$; Figure 2C).

Experiment 3. We previously showed that activation of the cAMP-PKA signal potentiates SF-1 transactivation by modifying the interactions between SF-1 and its cofactors, and PKA-induced activation of ArPII requires SF-1 (Fan et al. 2004). We studied whether any other environmental contaminants affected PKA-enhanced SF-1–mediated ArPII expression. In a luciferase reporter system, in which the 4.0-kb human ArPII luciferase reporter and pcDNA3.1-hSF-1 were coexpressed in NIH-3T3 fibroblast cells, 55 known environmental hormone chemicals were screened; among them, atrazine and the related triazine, simazine, stimulated the forskolin-enhanced SF-1–mediated ArPII expression by a factor of two to three (ANOVA, $p < 0.05$; Figure 3). As shown in Figure 2, the results were repeated and confirmed in the absence of forskolin. A third chemical, benzopyrene, also significantly induced luciferase ($p < 0.05$) but was less potent than the two triazines. Nonylphenol, di-*n*-butyl phthalate (DBP), dicyclohexylpthalate (DCHP), fenevalerate, and octylphenol all decreased luciferase activity (ANOVA, $p < 0.05$; Figure 3).

Experiment 4. Adeno-SF-1–infected KGN ovarian granulosa cells had an elevated basal level of aromatase expression (ANOVA, $p < 0.05$) and showed a 3.78- and a 4.94-fold increase in responsiveness to atrazine and simazine, respectively (ANOVA, $p < 0.05$; Figure 4A). The control (adeno-lacZ) vector had no effect (ANOVA, $p > 0.05$; Figure 4A). Thus, exogenous SF-1 conferred aromatase responsiveness to atrazine and simazine in otherwise atrazine-nonresponsive KGN granulosa cells. Furthermore, adeno-SF-1–infected KGN ovarian granulosa cells showed a significant increase in aromatase activity (ANOVA, $p < 0.05$; Figure 4B) as determined by a tritium release assay. Thus, in line with the results of promoter assays shown in experiment 2, the mRNA expression of CYP19, as well as the

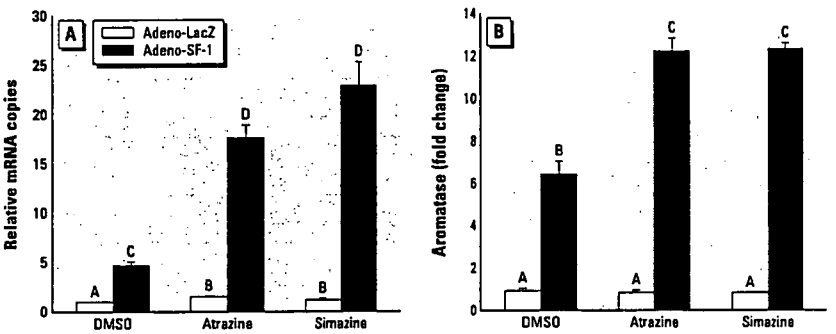

Figure 4. Effects of adeno-SF1 on responsiveness of KGN cells (mean ± SD) to 10^{-5} mol/L atrazine or 10^{-5} mol/L simazine. (*A*) Basal aromatase mRNA (*CYP19*; relative copies) was significantly increased in cells transfected with adeno-SF-1 relative to controls infected with adeno-LacZ. (*B*) Aromatase enzymatic activity (fold change) also increased in response to atrazine or simazine in adeno-SF-1 infected KGN cells, but not in the control adeno-LacZ infected cells. Letters above bars indicate statistical groups (ANOVA, $p < 0.05$).

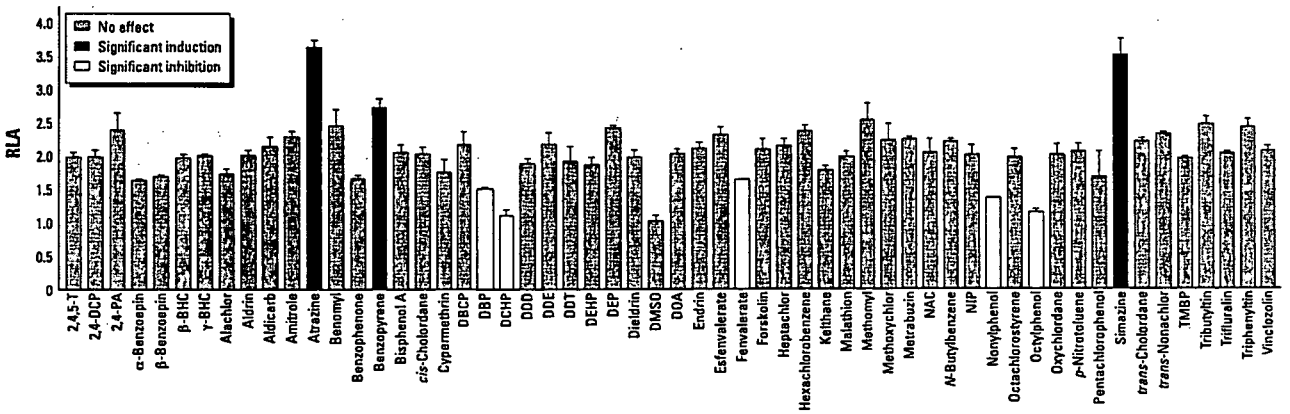

Figure 3. RLA (mean ± SD) of endocrine disruptors that affect forskolin-enhanced SF-1–mediated ArPII presented as chemicals with no effect on luciferase activity, those with significantly induced luciferase activity, or those with significantly inhibited luciferase activity as determined by ANOVA, followed by Fisher's protected least-significant-difference post hoc test ($p < 0.05$). Abbreviations: 2,4-DCP, 2,4-dichlorophenol; 2,4-PA, 2,4-dichlorophenoxy acetic acid; BHC, benzene hexachloride; DBCP, dibromochloropropane; DDD, 1,1-dichloro-2,2-bis(4-chlorophenyl)ethane; DDE, 1,1-dichloro-2-(*p*-chlorophenyl)-2-(*o*-chlorophenyl)ethylene; DDT, 1,1,1-trichloro-2,2-bis(4-chlorophenyl)ethane; DEHP, di-2-(ethyl-hexyl)-phthalate; DOA, dioctyl adipate; NAC, *N*-acetylcysteine; NIP, dinitrophenyl-phosphorothioate; TMBP, 4-(1,1,3,3- tetramethylbutyl) phenol. All chemicals were examined at ecologically relevant concentrations: 10^{-5} mol/L for all chemicals, except tributyltin and triphenyltin, which were examined at 10^{-7} mol/L.

enzymatic activities of aromatase, becomes responsive to both atrazine and simazine when SF-1 is exogenously expressed in KGN cells, which are otherwise atrazine nonresponsive.

Experiment 5. ArPII DNA sequences in the chromatin immunoprecipitates were significantly enriched by either simazine or atrazine, demonstrating that the triazines enhanced binding of SF-1 to ArPII (ANOVA, $p < 0.05$; Figure 5A, B). The responsiveness to atrazine and simazine was well-preserved when ArPII was reduced to 516 bp; however, when the SF-1 binding site (AGGTCA) was mutated to ATTTCA (a treatment that impairs SF-1 binding to ArPII), the responsiveness to atrazine and simazine was eliminated (ANOVA, $p < 0.05$; Figure 5C).

Experiment 6. The known SF-1 ligand 16PC was examined as a positive control for comparison with atrazine and two negative controls (*p*-nitrotoluene and benzophenone). A dose-dependent interaction between the control ligand (16PC) and immobilized SF-1 was observed by SPR (Figure 6A). Of the test ligands, only atrazine caused a significant (Figure 6B) and dose-dependent SPR response (Figure 6C). A quartz-crystal microbalance study confirmed that both 16PC and atrazine bound SF-1, whereas the solvent and negative control *p*-nitrotoluene did not (Figure 6D). The atrazine response was significantly lower than the positive control (16PC), but experiments such as scintillation proximity assays using radioactively labeled atrazine are required to determine the precise dissociation constant.

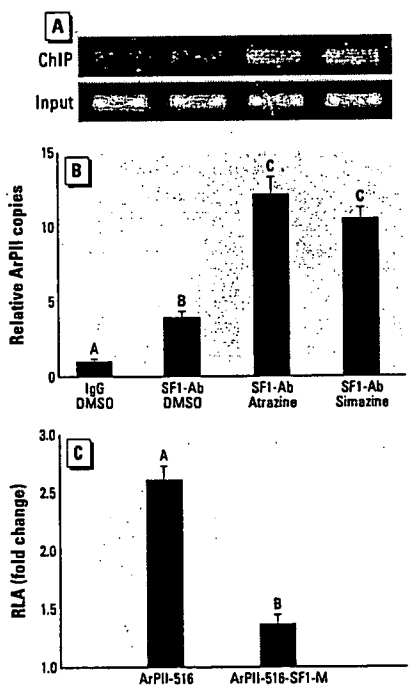

Figure 5. Effects of atrazine and simazine (10^{-5} mol/L) on SF-1 binding to ArPII. Atrazine and simazine enhanced SF-1–ArPII interactions in H295R cells as determined by common PCR (28 cycles; *A*) and as quantified by real-time PCR (*B*); mutation of the SF-1 binding site on ArPII significantly reduced responsiveness to atrazine. The responsiveness to atrazine and simazine was well preserved when ArPII was reduced to 516 bp (ArPII-516), but responsiveness was lost when the SF-1 binding site was mutatated to ATTTCA (ArPII-516-SF1-M) (*C*). In (*B*) and (*C*), bars show mean ± SD. Letters above bars indicate statistical groups (ANOVA, $p < 0.05$).

Discussion

Atrazine increases aromatase by binding to and inhibiting phosphodiesterase (Roberge et al. 2004; Sanderson et al. 2000, 2001), resulting in elevated cAMP. Elevated cAMP results in increased transcription of *CYP19*, increased aromatase activity, and ultimately increased estrogen production. Although the effects of atrazine on aromatase vary between cell lines and tissues, the current study explains this variation. There are six tissue- and cell-specific aromatase promoters in humans. Atrazine affects aromatase expression only in cell and tissue types that use the SF-1–dependent ArPII promoter. Tissue types and cell lines that do not respond to atrazine are those types that do not utilize ArPII or that do not express SF-1.

In addition to elucidating the role of SF-1 in atrazine-induced aromatase expression and explaining variation in responses between cell types, we developed an assay for detecting endocrine disruption via aromatase induction and for distinguishing chemicals that alter aromatase activity from those that alter aromatase expression. We confirmed that atrazine and simazine induce aromatase, consistent with the literature (Heneweer et al. 2004; Sanderson et al. 2000, 2001, 2002). The reduction in aromatase by phthalates (DCHP and DBP) and octylphenol is consistent with their previously reported reduction in estrogen synthesis (Davis et al. 1994; Kim et al. 2003; Lovekamp and Davis 2001). Vinclozolin (which had no effect in the present study) increases aromatase, but at concentrations 10 times higher than used here (Sanderson et al. 2002). The other chemicals examined have not been previously examined for effects on aromatase.

The role of SF-1 we identified in the present study is important. Orphan receptors, such as SF-1, bind their response elements and regulate transcription constitutively, but ligand-binding may enhance their activity. To date, only phospholipids (Krylova et al. 2005; Li et al. 2005) have been identified as endogenous ligands for SF-1. Here, we show that atrazine not only elevates cAMP, which also increases SF-1 expression (Heneweer et al. 2004; Lehmann et al. 2005; Roberge et al. 2004; Sanderson et al. 2000), but also binds SF-1 and increases its interaction with ArPII.

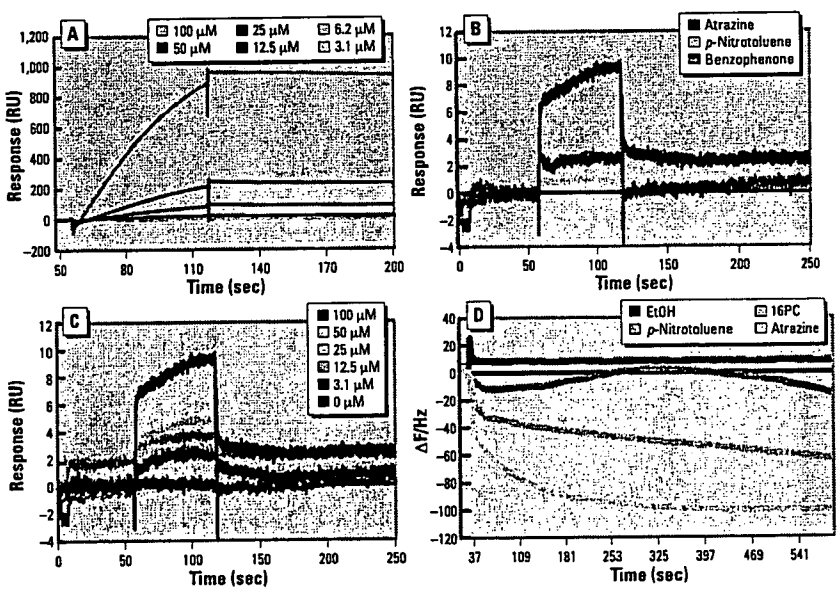

Figure 6. Kinetic analysis of atrazine binding to SF-1 protein as analyzed by SPR [changes in mass concentration are detected as differences in the refractive index and shown in resonance units (RU)]. (*A*) Sensorgrams of six concentrations of 16PC (the positive control ligand) added to SF-1. (*B*) Sensorgrams showing atrazine, benzophenone, or *p*-nitrotoluene (100 µM each) binding to immobilized SF-1 (only atrazine caused a significant response). (*C*) Sensorgrams of six concentrations of atrazine added to the immobilized SF-1 (note the dose-dependent response). (*D*) Sensorgrams showing interactions between atrazine and SF-1 on a quartz-crystal microbalance. 16PC caused a clear decrease in frequency, demonstrating binding between the ligand and SF-1; atrazine also substantially decreased the frequency, but ethanol (EtOH) and the negative control *p*-nitrotoluene did not.

The findings of the present study are important for understanding the negative impact that atrazine contamination has on both environmental and public health. In addition to its vital roles in the reproductive system, the atrazine-responsive ArPII is also critically involved in breast cancer oncogenesis. The role of estrogen in breast cancer and the potential role of atrazine exposure is consistent with increased plasma estrogen levels in several strains of rats when exposed to atrazine (Eldridge and Wetzel 1999; Eldridge et al. 1994a, 1994b; Stevens et al. 1994; Stoker et al. 2000; Wetzel et al. 1994) and the increased incidence of estrogen-dependent mammary cancers in rodents (Eldridge et al. 1994a; Stevens et al. 1994; Wetzel et al. 1994). Further, Ueda et al. (2005) showed that atrazine-induced tumors in rodents are estrogen-receptor positive. The findings in rodents are consistent with increased aromatase expression and activity in human cell lines in the present study and in previous studies (Heneweer et al. 2004, Sanderson et al. 2000, 2001) and in human tissues (Roberge et al. 2004). The estrogen that stimulates breast cancer growth in humans is derived from both ovarian and extraovarian sources. Local estrogen production, which contributes to hormonal stimulation of breast cancers in breast adipose tissue and fibroblasts, is also dependent on ArPII (Bulun et al. 2005). This extraovarian estrogen plays a profound mitogenic role in breast tumors (Bulun et al. 2005): Local estrogen levels in breast tumors can be 10 times higher than that in the circulation of postmenopausal women (Van Landeghem et al. 1985), likely due to a critical shift in promoter usage from I.4 (used in normal adipose tissue) to ArPII (abnormally activated in breast adipose tissue containing a tumor) (Agarwal et al. 1996; Harada et al. 1993). Although normal breast tissue does not typically utilize ArPII, once transformed, breast cancer cells (malignant epithelial cells) induce use of ArPII in adjacent fibroblasts (Agarwal et al. 1996; Harada et al. 1993; Utsumi et al. 1996; Zhou et al. 1996). In this regard, the ability of atrazine to stimulate ArPII is extremely significant. Atrazine increases the incidence of mammary cancer in rodents (Eldridge et al. 1994a; Stevens et al. 1994; Wetzel et al. 1994), and at least one cohort study in humans showed that atrazine is associated with breast cancer in women whose well water is contaminated with atrazine (Kettles et al. 1997).

Atrazine induces prostatitis (Stoker et al. 1999) and prostate cancer in rats (Pintér et al. 1980) and was also associated with an 8.4-fold increase in prostate cancer in men working in an atrazine production facility in San Gabriel, Louisiana (Maclennan et al. 2002; Sass 2003). Although typically considered androgen dependent, prostate cancer is also estrogen dependent and is associated with increased local estrogen production (Christensen and Lephart 2004; Ellem et al. 2004; Härkönena and Mäkelä 2004). Aromatase expression and activity are low in normal prostate cells, but in malignant cells in the prostate, they increase to levels comparable with those observed in breast cancer (Prins and Birch 1997). This aromatase activity is associated exclusively with the atrazine-regulated ArPII and renders the popular antiandrogen treatments for prostate cancer useless (Ellem et al. 2004). Also, low levels of estrogen, when bound to estrogen receptor-α (ER-α), result in proliferation of the prostate (Ellem et al. 2004). Thus, in prostate cancer, induction of aromatase via ArPII in prostate epithelia results in estrogen synthesis that, in turn, affects the prostate epithelia in an autocrine/intracrine fashion via binding to ER-α. Further, elevated estrogens during early development inhibit prostate growth but predispose individuals to prostate disease later in life (Prins and Birch 1997; Pylkkanen et al. 1993).

In addition to atrazine's contribution to adverse health outcomes in humans, the effect of atrazine on cells and tissues that utilize ArPII is also significant, because all vertebrates utilize ArPII during gonadal differentiation and development (Simpson et al. 1994, 2002). In fact, the activity of atrazine and simazine at 10^{-7} M (21.57 mol/L) in the present study is in the range that chemically castrates and feminizes male amphibians (0.1–20 ppb; 1 ppb = 1 mol/L) (Carr et al. 2003; Hayes 2004, 2005; Hayes et al. 2002a, 2002b, 2003, 2006a, 2006b; McKoy et al. 2002; Miyahara et al., unpublished data; Reeder et al. 1998; Tavera-Mendoza et al. 2002) and fish (6 ppb) (Moore and Waring 1998). Thus, the present study is also significant because the effects in wildlife likely occur through the same molecular mechanisms as documented here; however, the cell lines and molecular tools are not available for wildlife species to examine these effects on this same level.

Considering the prevalence of atrazine in the environment, the continued rise of cancer as the leading cause of death in the United States (breast cancer and prostate cancer are the most common cancers in men and women, respectively), the present findings raise concern for the impact of atrazine on environmental and public health. This is especially troubling because African Americans and Hispanic Americans, more likely to be occupationally exposed to pesticides and less likely to have proper access to health care, are two to four times more likely to die from breast and prostate cancer, respectively.

The fact that aromatase inhibitors have proven effective at treating breast cancer induced by adipose aromatase (Brodie et al. 1999) and promise to have similar therapeutic value in endometriosis (Shippen and West 2004) underscores the potential role that atrazine (an aromatase inducer) plays in increasing the risk of these diseases: Aromatase expression and estrogen production is exclusively regulated by ArPII and is SF-1 dependent in endometriosis, a disease that affects 4–6 million women (10% of American women) per year (Bulun et al. 2005). Further, overexpression of aromatase plays a role in other diseases including uterine fibroids (uterine leiomyomata), aromatase overexpression syndrome (Bulun et al. 2005), and polycystic ovarian syndrome (Pierro et al. 1997). The many mammalian tissues and cell types that express SF-1 (and use ArPII) are shown in Table 1. Given the ubiquity of atrazine contamination, atrazine's persistence in the environment, and the concern for effects of

Table 1. Summary of mammalian tissues and cells that show cAMP/SF-1 dependent, ArPII-like expression of aromatase.

Tissue/cell type	References
Rat ovary (granulosa)	Carlone and Richards 1997; Falender et al. 2003; Fitzpatrick and Richards 1994; Lynch et al. 1993
Rat R2C (Leydig cell carcinoma)	Carlone and Richards 1997; Falender et al. 2003; Fitzpatrick and Richards 1994
Rat H540 (Leydig tumor cells)	Young and McPhaul 1997
Human prostate stroma	Ellem et al. 2004
Human prostate tumor (epithelial cells)	Ellem et al. 2004
Human LNCaP (prostate cancer cells)	Ellem et al. 2004
Human Sertoli cells	Gurates et al. 2002
Human endometrial stroma	Gurates et al. 2003
Human corpus luteum	Michael et al. 1995
Human preovulatory follicles	Simpson et al. 1994
Human ovary (granulosa)	Bulun et al. 2005; Sanderson et al. 2000
Human adipose tissue fibroblast	Bulun et al. 2005
Human breast tumor fibroblast	Bulun et al. 2005
Human malignant epithelial cells	Bulun et al. 2005
Human breast cancer adipose tissue	Bulun et al. 2005
Human extra-ovarian endometrium	Bulun et al. 2005
Human ovary-derived endometrial cells	Gurates et al. 2003
Human H295R (adrenal corticocarcinoma)	Sanderson et al. 2000

endocrine-disrupting chemicals in wildlife, especially in amphibian declines (Hayes et al. 2002a, 2002b, 2003, 2006a, 2006b), and in cancer (Kettles et al. 1997; Maclennan et al. 2002; Sass 2003), the findings reported here are quite significant. This concern was voiced several years ago (Sanderson et al. 2000):

> A logical concern would be that exposure to triazine herbicides, which are produced and used in large quantities, and are ubiquitous environmental contaminants, may similarly contribute to estrogen-mediated toxicities and inappropriate sexual differentiation.

References

Agarwal V, Ashanullah C, Simpson E, Bulun S. 1996. Use of alternative promoters to express the aromatase cytochrome P450 (*CYP19*) gene in breast adipose tissue of cancer-free and breast cancer patients. J Clin Endocrinol Metab 81:3843–3849.

Babic-Gojmerac T, Kniewald Z, Kniewald J. 1989. Testosterone metabolism in neuroendocrine organs in male rats under atrazine and deethylatrazine influence. J Steroid Biochem 33:141–146.

Brodie A, Lu Q, Liu Y, Long B. 1999. Aromatase inhibitors and their antitumor effects in model systems. Endocr Relat Cancer 6:205–210.

Bulun S, Lin Z, Imir G, Amin S, Demura M, Yilmaz B, et al. 2005. Regulation of aromatase expression in estrogen-responsive breast and uterine disease: from bench to treatment. Pharmacol Rev 57:359–383.

Carlone D, Richards J. 1997. Evidence that functional interactions of CREB and SF-1 mediate hormone regulated expression of the aromatase gene in granulosa cells and constitutive expression in R2C cells. J Steroid Biochem Mol Biol 61:223–231.

Carr J, Gentles A, Smith E, Goleman W, Urquidi L, Thuett K, et al. 2003. Response of larval *Xenopus laevis* to atrazine: assessment of growth, metamorphosis, and gonadal and laryngeal morphology. Environ Toxicol Chem 22:396–405.

Cooper RL, Stoker TE, McElroy WK. 1999. Atrazine (ATR) disrupts hypothalamic catecholamines and pituitary function. Toxicologist 42:60–66.

Cooper RL, Stoker TE, Tyrey L, Goldman JM, McElroy WK. 2000. Atrazine disrupts the hypothalamic control of pituitary-ovarian function. Toxicol Sci 53:297–307.

Crain D, Guillette LJ, Rooney AA, Pickford D. 1997. Alterations in steroidogenesis in alligators (*Alligator mississippiensis*) exposed naturally and experimentally to environmental contaminants. Environ Health Perspect 105:528–533.

Cummings A, Rhodes B, Cooper R. 2000. Effect of atrazine on implantation and early pregnancy in 4 strains of rats. Toxicol Sci 58:135–143.

Davis B, Weaver R, Gaines L, Heindel J. 1994. Mono-(2-ethylexyl) phthalate suppresses estradiol production independent of FSH-cAMP stimulation in rat granulosa cells. Toxicol Appl Pharmacol 128:224–228.

Eldridge J, Fleenore-Heyser D, Extron P, Wetzel L, Breckenridge C, Gillis J, et al. 1994a. Short-term effects of chlorotriazines on estrus in female Sprague-Dawley and Fischer 344 rats. J Toxicol Environ Health 43:155–167.

Eldridge JC, Tennant MK, Wetzel LT, Breckenridge CB, Stevens JT. 1994b. Factors affecting mammary tumor incidence in chlorotriazine-treated female rats: hormonal properties, dosage, and animal strain. Environ Health Perspect 102(suppl 11):29–36.

Eldridge JC, Wetzel LT, Tyrey L. 1999. Estrous cycle patterns of Sprague-Dawley rats during acute and chronic atrazine administration. Reprod Toxicol 13:491–498.

Ellem S, Schmitt J, Pedersen J, Frydenberg M, Risbridger G. 2004. Local aromatase expression in human prostate is altered in malignancy. J Clin Endocrinol Metab 89:2434–2441.

Falender A, Lanz R, Malenfant D, Belanger N, Richards J. 2003. Differential expression of steroidogenic factor-1 and FTF/LRH-1 in the rodent ovary. Endocrinology 144:3598–3610.

Fan W, Yanase T, Morinaga H, Mu Y, Nomura M, Okabe T, et al. 2005a. Activation of peroxisome proliferator-activated receptor-gamma and retinoid X receptor inhibits aromatase transcription via nuclear factor-kappa B. Endocrinology 146:85–92.

Fan W, Yanase T, Nomura M, Okabe T, Goto K, Sato T, et al. 2005b. Androgen receptor null male mice develop late-onset obesity caused by decreased energy expenditure and lipolytic activity but show normal insulin sensitivity with high adiponectin secretion. Diabetes 54:1000–1008.

Fan W, Yanase T, Wu Y, Kawate H, Saitoh M, Oba K, et al. 2004. Protein kinase A potentiates adrenal 4 binding protein/steroidogenic factor 1 transactivation by reintegrating the subcellular dynamic interactions of the nuclear receptor with its cofactors, general control nonderepressed-5/transformation/transcription domain-associated protein, and suppressor, dosage-sensitive sex reversal-1: a laser confocal imaging study in living KGN cells. Mol Endocrinol 18:127–141.

Fenelon J, Moore R. 1998. Transport of agrichemicals to ground and surface waters in a small central Indiana watershed. J Environ Qual 27:884–894.

Fitzpatrick S, Richards J. 1994. Identification of a cyclic adenosine 3',5'-monophosphate-response element in the rat aromatase promoter that is required for transcriptional activation in rat granulosa cells and R2C Leydig cells. Mol Endocrinol 8:1309–1319.

Frank R, Sirons G. 1979. Atrazine: its use in corn production and its loss to stream waters in southern Ontario. Sci Total Environ 12:223–239.

Friedmann A. 2002. Atrazine inhibition of testosterone production in rat males following peripubertal exposure. Reprod Toxicol 16:275–279.

Genbank. 2007. GenBank Overview. Available: http://www.ncbi.nlm.nih.gov/Genbank/index.html [accessed 30 March 2007].

Gondo S, Yanase T, Okabe T, Tanaka T, Morinaga H, Nomura M, et al. 2004. SF-1/Ad4BP transforms primary long-term cultured bone marrow cells into ACTH-responsive steroidogenic cells. Genes Cells 12:1239–1247.

Gurates B, Amsterdam A, Tamura M, Yang S, Zhou J, Fang Z, et al. 2003. WT1 and DAX-1 regulate SF-1-mediated human P450arom gene expression in gonadal cells. Molec Cell Endocrinol 208:61–75.

Gurates B, Sebastin S, Yang S, Zhou J, Mitsutoshi T, Fang Z, et al. 2002. WT1 and DAX-1 inhibit aromatase P450 expression in human endometrial and endometriotic stromal cells. J Clin Endocrinol Metab 87:4369–4377.

Harada N, Utsumi T, Takagi Y. 1993. Tissue-specific expression of the human aromatase cytochrome P450 gene by alternative use of multiple exons I and promoters and switching of tissue-specific exons I in carcinogenesis. Proc Natl Acad Sci USA 90:11312–11316.

Härkönena P, Mäkelä S. 2004. Role of estrogens in development of prostate cancer. J Steroid Biochem 92:297–305.

Hayes T. 2004. There is no denying this: defusing the confusion about atrazine. Bioscience 54:1138–1149.

Hayes T. 2005. Welcome to the revolution: integrative biology and assessing the impact of endocrine disruptors on environmental and public health. J Integrative Comp Biol 45:321–329.

Hayes T, Collins A, Lee M, Mendoza M, Noriega N, Stuart AA, et al. 2002a. Hermaphroditic, demasculinized frogs after exposure to the herbicide atrazine at low ecologically relevant doses. Proc Natl Acad Sci USA 99:5476–5480.

Hayes T, Haston K, Tsui M, Hoang A, Haeffele C, Vonk A. 2002b. Feminization of male frogs in the wild. Nature 419:895–896.

Hayes T, Haston K, Tsui M, Hoang A, Haeffele C, Vonk A. 2003. Atrazine-induced hermaphroditism at 0.1 ppb in American leopard frogs (*Rana pipiens*): laboratory and field evidence. Environ Health Perspect 111:568–575.

Hayes TB, Case P, Chui S, Chung D, Haefele C, Haston K, et al. 2006a. Pesticide mixtures, endocrine disruption, and amphibian declines: are we underestimating the impact? Environ Health Perspect 114(suppl 1):40–50.

Hayes TB, Stuart AA, Mendoza M, Collins A, Noriega N, Vonk A, et al. 2006b. Characterization of atrazine-induced gonadal malformations in African clawed frogs (Xenopus laevis) and comparisons with effects of an androgen antagonist (cyproterone acetate) and exogenous estrogen (17β-estradiol): support for the demasculinization/feminization hypothesis. Environ Health Perspect 114(suppl 1):134–141.

Heneweer M, van den Berg M, Sanderson J. 2004. A comparison of human H295R and rat R2C cell lines as *in vitro* screening tools for effects on aromatase. Toxicol Lett 146:183–194.

Keller J, McClellan-Green P. 2004. Effects of organochlorine compounds on cytochrome P450 aromatase activity in an immortal sea turtle cell line. Mar Environ Res 58:347–351.

Kettles MA, Browning SR, Prince TS, Hostman SW. 1997. Triazine exposure and breast cancer incidence: an ecologic study of Kentucky counties. Environ Health Perspect 105:1222–1227.

Kim H, Saito K, Ishizuka M, Kazusaka A, Fujita S. 2003. Short period exposure to di-(2-ethylhexyl) phthalate regulates testosterone metabolism in testis of prepubertal rats. Arch Toxicol 77:446–451.

Kniewald J, Mildner P, Kniewald Z. 1979. Effects of s-triazine herbicides on 5α-dihydrotestosterone receptor complex formation, 5α-reductase and 3β-hydroxysteroid dehydrogenase activity at the anterior pituitary level. J Steroid Biochem 11:833–838.

Kniewald J, Mildner P, Kniewald Z. 1980. Effects of s-triazine herbicides on 5α-dihydrotestosterone receptor complex formation in the hypothalamus and ventral prostate. In: Pharmacological Modulation of Steroid Action (Genazzani E, DiCarlo F, Mainwaring WIP, eds). New York:Raven Press, 159–169.

Kniewald J, Osredecki V, Gojmerac T, Zechner V, Kniewald Z. 1995. Effect of s-triazine compounds on testosterone metabolism in the rat prostate. J Appl Toxicol 15:215–218.

Kolpin D, Barbash J, Gilliom R. 1998. Occurence of pesticides in shallow groundwater of the United States: initial results from the National Water-Quality Assessment Program. Environ Sci Technol 32:558–566.

Komatsu T, Mizusaki H, Mukai T, Ogawa H, Baba D, Shirakawa M, et al. 2004. Small ubiquitin-like modifier 1 (SUMO-1) modification of the synergy control motif of Ad4 binding protein/steroidogenic factor 1 (Ad4BP/SF-1) regulates synergistic transcription between Ad4BP/SF-1 and Sox9. Mol Endocrinol 18:2451–2462.

Krylova I, Sablin E, Moore J, Xu R, Waitt G, MacKay J, et al. 2005. Structural analyses reveal phosphatidyl inositols as ligands for the NR5 orphan receptors SF-1 and LRH-1. Cell 120:343–355.

Lehmann TP, Biernacka-Lukanty JM, Saraco N, Langlois D, Li JY, et al. 2005. Temporal pattern of the induction of SF-1 gene expression by the signal transduction pathway involving 3',5'-cyclic adenosine monophosphate. Acta Biochimica Polonica 52:485–491.

Li Y, Choi M, Cavey G, Daugherty J, Suino K, Kovach A, et al. 2005. Crystallographic identification and functional characterization of phospholipids as ligands for the orphan nuclear receptor steroidogenic factor-1. Mol Cell 17:491–502.

Lode O, Eklo O, Holen B, Svensen A, Johnsen A. 1995. Pesticides in precipitation in Norway. Sci Total Environ 160/161:421–431.

Lovekamp T, Davis B. 2001. Mono-(2-ethylhexyl) phthalate suppresses aromatase transcript levels and estradiol production in cultured rat granulosa cells. Toxicol Appl Pharmacol 172:217–224.

Lynch JP, Lala DS, Peluso JJ, Luo W, Parker KL, White BA. 1993. Steroidogenic factor 1, an orphan nuclear receptor, regulates the expression of the rat aromatase gene in gonadal tissues. Mol Endocrinol 7:776–786.

Maclennan PA, Delzell E, Sathiakumar N, Myers SL, Cheng H, Grizzle W, et al. 2002. Cancer incidence among triazine herbicide manufacturing workers. J Occup Environ Med 44:1048–1058.

McCoy K, Sepulveda M, Gross T. 2002. Atrazine exposure and reproductive system abnormalities in field collected *Bufo marinus* (Abstract). In: SETAC 2002, 16–20 November 2002, Salt Lake City, UT. Available: http://abstracts.co.allenpress.com/pweb/setac2002/document/?ID=20061 [accessed 27 March 2007].

Michael M, Kilgore M, Morohashi K, Simpson E. 1995. Ad4BP/DF-1 regulates cyclic AMP-induced transcription from the proximal promoter (PII) of the human aromatase P450 (*CYP19*) gene in the ovary. J Biol Chem 270:13561–13566.

Miller S, Sweet C, Depinto J, Hornbuckle K. 2000. Atrazine and nutrients in precipitation: results from the Lake Michigan mass balance study. Environ Sci Technol 34:55–61.

Moore A, Waring C. 1998. Mechanistic effects of a triazine pesticide on reproductive endocrine function in mature male Atlantic salmon (*Salmo salar* L.) parr. Pesticide Biochem Physiol 62:41–50.

Morinaga H, Yanase T, Nomura M, Okabe T, Goto K, Harada N, et al. 2004. A benzimidazole fungicide, benomyl, and its metabolite, carbendazim, induce aromatase activity in a human ovarian granulose-like tumor cell line (KGN). Endocrinology 145:1860–1869.

Mu Y, Yanase T, Nishi Y, Waseda N, Oda T, Tanaka A, et al. 2000. Insulin sensitizer, troglitazone, directly inhibits aromatase activity in human ovarian granulosa cells. Biochem Biophys Res Commun 271:710–713.

Müller S, Berg M, Ulrich M, Schwarzenbach RP. 1997. Atrazine

and its primary metabolites in Swiss lakes: input characteristics and long-term behavior in the water column. Environ Sci Technol 31:2104–2113.

Narotsky M, Best DS, Guidici DL, Cooper RL. 2001. Strain comparisons of atrazine-induced pregnancy loss in the rat. Reprod Toxicol 15:61–69.

Nishi Y, Yanase T, Mu Y, Oba K, Ichino I, Saito M, et al. 2001. Establishment and characterization of a steroidogenic human granulosa-like tumor cell line, KGN, that expresses functional follicle-stimulating hormone receptor. Endocrinology 142:437–445.

Oba K, Yanase T, Ichino I, Goto K, Takayanagi R, Nawata H. 2000. Transcriptional regulation of the human FTZ-F1 gene encoding Ad4BP/SF-1. J Biochem (Tokyo) 128:517–528.

Pierro E, Andreani C, Lazzarin N, Cento R, Lanzone A, Caruso A, et al. 1997. Further evidence of increased aromatase activity in granulosa luteal cells from polycystic ovary. Hum Reprod (Oxford) 12:1890–1896.

Pintér A, Torok G, Borzsonyi M, Surjan A, Csik M, Kelecsenyi Z, et al. 1980. Long-term carcinogenicity bioassay of the herbicide atrazine in F344 rats. Neoplasma 37:533–544.

Prins G, Birch L. 1997. Neonatal estrogen exposure up-regulates estrogen receptor expression in the developing and adult rat prostate lobes. Endocrinology 138:1801–1809.

Pylkkanen L, Makela S, Valve E, Toikkanen S, Santti R. 1993. Prostatic dysplasia associated with increased expression of c-myc in neonatally estrogenized mice. J Urol 149:1593–1601.

Reeder A, Foley G, Nichols D, Hansen L, Wikoff B, Faeh S, et al. 1998. Forms and prevalence of intersexuality and effects of environmental contaminants on sexuality in cricket frogs (*Acris crepitans*). Environ Health Perspect 106:261–266.

Roberge M, Hakk H, Larsen G. 2004. Atrazine is a competitive inhibitor of phosphodiesterase but does not affect the estrogen receptor. Toxicol Lett 154:61–68.

Rubin G, Duong J, Clyne C, Speed C, Murata Y, Gong C, et al. 2002. Ligands for the peroxisomal proliferator-activated receptor gamma and the retinoid X receptor inhibit aromatase cytochrome P450 (*CYP19*) expression mediated by promoter II in human breast adipose. Endocrinology 143:2863–2871.

Sanderson JT, Boerma J, Lansbergen G, van den Berg M. 2002. Induction and inhibition of aromatase (*CYP19*) activity by various classes of pesticides in H295R human adrenocortical carcinoma cells. Toxicol Appl Pharmacol 182:44–54.

Sanderson JT, Letcher RJ, Heneweer M, Giesy JP, van den Berg M. 2001. Effects of chloro-*s*-triazine herbicides and metabolites on aromatase activity in various human cell lines and on vitellogenin production in male carp hepatocytes. Environ Health Perspect 109:1027–1031.

Sanderson JT, Seinen W, Giesy JP, van den Berg M. 2000. 2-Chloro-triazine herbicides induce aromatase (*CYP19*) activity in H295R human adrenocortical carcinoma cells: a novel mechanism for estrogenicity? Toxicol Sci 54:121–127.

Sass J. 2003. Letter to the editor: Cancer Incidence Among Tiazine Herbicide Manufacturing Workers. J Occup Environ Med 45:343–344.

Shafer TJ, Ward TR, Meacham CA, Cooper RL. 1999. Effects of the cholorotriazine herbicide, cyanizine on GABAA receptors in cortical tissue from rat brain. Toxicology 142:57–68.

Shippen E, West W. 2004. Successful treatment of severe endometriosis in two premenopausal women with an aromatase inhibitor. Fertil Steril 81:1395–1398.

Šimic B, Kniewald Z, Davies J, Kniewald J. 1991. Reversibility of inhibitory effect of atrazine and lindane on 5-dihydrotestosterone receptor complex formation in rat prostate. Bull Environ Contam Toxicol 46:92–99.

Simpson E, Clyne C, Rubin G, Boon W, Robertson K, Britt K, et al. 2002. Aromatase—a brief overview. Annu Rev Physiol 64:93–127.

Simpson E, Mahendroo M, Means G, Kilgore M, Hinshelwood M, Graham-Lorence S, et al. 1994. Aromatase cytochrome P450, the enzyme responsible for estrogen biosynthesis. Endocr Rev 15:342–355.

Solomon K, Baker D, Richards R, Dixon K, Klaine S, LaPoint T, et al. 1996. Ecological risk assessment of atrazine in North American surface waters. Environ Toxicol Chem 15:31–76.

Spano L, Tyler C, van Aerle R, Devos P, Mandiki S, Silvestre F, et al. 2004. Effects of atrazine on sex steroid dynamics, plasma vitellogenin concentration and gonad development in adult goldfish (*Carassius auratus*). Aquat Toxicol (Amsterdam) 66:369–379.

Stevens JT, Breckenridge CB, Wetzel LT, Gillis JH, Luempert LG III, Eldridge JC. 1994. Hypothesis for mammary tumorigenesis in Sprague-Dawley rats exposed to certain triazine herbicides. J Toxicol Environ Health 43:139–153.

Stoker TE, Laws S, Guidici D, Cooper R. 2000. The effect of atrazine on puberty in male Wistar rats: an evaluation in the protocol for the assessment of pubertal development and thyroid function. Toxicol Sci 58:50–59.

Stoker TE, Robinette CL, Cooper RL. 1999. Maternal exposure to atrazine during lactation suppresses suckling-induced prolactin release and results in prostatitis in the adult offspring. Toxicol Sci 52:68–79.

Tavera-Mendoza L, Ruby S, Brousseau P, Fournier M, Cyr D, Marcogliese D. 2002. Response of the amphibian tadpole (*Xenopus laevis*) to atrazine during sexual differentiation of the testis. Environ Toxicol Chem 21:527–531.

Tennant MK, Hill DS, Eldridge JC, Wetzel LT, Breckenridge CB, Stevens JT. 1994. Chloro-*s*-triazine antagonism of estrogen action: limited interaction with estrogen receptor binding. J Toxicol Environ Health 43:197–211.

Thurman E, Cromwell A. 2000. Atmospheric transport, deposition, and fate of triazine herbicides and their metabolites in pristine areas at Isle Royale National Park. Environ Sci Technol 34:3079–3085.

Ueda M, Imai T, Takizawa T, Onodera H, Mitsumori K, Matsui T, et al. 2005. Possible enhancing effects of atrazine on growth of 7,12-dimethylbenz(*a*)anthracene induced mammary tumors in ovariectomized Sprague-Dawley rats. Cancer Sci 96:19–25.

UniGene. 2007. Available: http://www.ncbi.nlm.nih.gov/entrez/query.fcgi?db=unigene [accessed 30 March 2007].

Utsumi T, Harada N, Maruta M, Takagi Y. 1996. Presence of alternatively spliced transcripts of aromatase gene in human breast cancer. J Clin Endocrinol Metab 81:2344–2349.

Van Landeghem AA, Poortman J, Nabuurs M, Thijssen JH. 1985. Endogenous concentration and subcellular distribution of estrogens in normal and malignant human breast tissue. Cancer Res 45:2900–2906

Wetzel LT, Luempert LG III, Breckenridge CB, Tisdel MO, Stevens JT, Thakur AK, et al. 1994. Chronic effects of atrazine on estrus and mammary gland formation in female Sprague-Dawley and Fischer-344 rats. J Toxicol Environ Health 43:169–182.

Young M, McPhaul M. 1997. Definition of the elements required for the activity of the rat aromatase promoter in steroidogenic cell lines. J Steroid Biochem Mol Biol 61:341–348.

Zhou C, Zhou D, Estaban J, Murai J, Siiteri P, Wilczynski S, et al. 1996. Aromatase gene expression and its exon I usage in human breast tumors. Detection of aromatase messenger RNA by reverse transcription polymerase chain reaction. J Steroid Biochem Mol Biol 59:163–171.

MOLECULAR AND CELLULAR BIOLOGY, July 2007, p. 4807–4814 Vol. 27, No. 13
0270-7306/07/$08.00+0 doi:10.1128/MCB.02039-06

The Pituitary Function of Androgen Receptor Constitutes a Glucocorticoid Production Circuit[▽]

Junko Miyamoto,[1]† Takahiro Matsumoto,[1,2]† Hiroko Shiina,[1] Kazuki Inoue,[1] Ichiro Takada,[1] Saya Ito,[1] Johbu Itoh,[3] Takeo Minematsu,[4] Takashi Sato,[1] Toshihiko Yanase,[5] Hajime Nawata,[5] Yoshiyuki R. Osamura,[4] and Shigeaki Kato[1,2]*

Institute of Molecular and Cellular Biosciences, University of Tokyo, 1-1-1 Yayoi, Bunkyo-ku, Tokyo 113-0032, Japan[1]; ERATO, Japan Science and Technology Agency, 4-1-8 Honcho, Kawaguchisi, Saitama 332-0012, Japan[2]; Teaching and Research Support Center[3] and Department of Pathology,[4] Tokai University School of Medicine, Boseidai, Isehara, Kanagawa 259-1193, Japan; and Department of Medicine and Bioregulatory Science, Graduate School of Medical Sciences, Kyushu University, Fukuoka 812-8582, Japan[5]

Received 1 November 2006/Returned for modification 18 December 2006/Accepted 16 April 2007

Androgen receptor (AR) mediates diverse androgen actions, particularly reproductive processes in males and females. AR-mediated androgen signaling is considered to also control metabolic processes; however, the molecular basis remains elusive. In the present study, we explored the molecular mechanism of late-onset obesity in male AR null mutant (ARKO) mice. We determined that the obesity was caused by a hypercorticoid state. The negative feedback system regulating glucocorticoid production was impaired in ARKO mice. Male and female ARKO mice exhibited hypertrophic adrenal glands and glucocorticoid overproduction, presumably due to high levels of adrenal corticotropic hormone. The pituitary glands of the ARKO males had increased expression of proopiomelanocortin and decreased expression of the glucocorticoid receptor (GR). There were no overt structural abnormalities and no alteration in the distribution of cell types in the pituitaries of male ARKO mice. Additionally, there was normal production of the other hormones within the glucocorticoid feedback system in both the pituitary and hypothalamus. In a cell line derived from pituitary glands, GR expression was under the positive control of the activated AR. Thus, this study suggests that the activated AR supports the negative feedback regulation of glucocorticoid production via up-regulation of GR expression in the pituitary gland.

Sex steroid hormones exert a wide variety of biological actions. They are also involved in pathological events, such as the development of hormone-dependent cancers in reproductive organs (5, 37). In vertebrates, sex hormones play a pivotal role in male reproductive function and metabolic control. Most sex steroid actions are mediated through transcriptional control of target genes by nuclear receptors (NRs). NRs form a gene superfamily and act as transcriptional factors (9, 20). Sex hormone receptors have been shown to transactivate particular sets of target genes in a hormone-dependent manner through direct DNA binding to specific elements in target gene promoters. Hormone receptors activated by hormone binding recruit a number of coregulator-coregulator complexes for transactivation (28). These complexes then affect transcription through chromatin remodeling (12, 17, 22) and histone modification (1, 7). Hormone binding to the receptors may also transrepress target genes. The mechanisms of hormone-dependent transrepression of steroid receptors likely involve protein-protein interactions and are thus more diverse than that of transactivation (8, 10, 13, 21).

The molecular mechanisms behind the regulation of gene transcription by hormones and their NRs are complicated. Gene disruption studies have clarified the role of various NRs in steroid hormone action. By combining a Cre-loxP system with a canonical gene disruption approach, we succeeded in disrupting the androgen receptor (AR) on the X chromosome in mice in a manner that did not result in male infertility (14). Male AR null mutant (ARKO) mice exhibit abnormalities typical of testicular feminization mutants, including female external genitalia with atrophic testis and impaired sex behavior (29). Growth of the male ARKO mice is partially retarded, with impaired bone growth coupled with high bone turnover (16). The male mice also develop late-onset obesity (30). In contrast, no clear phenotypic abnormalities are present in female ARKO mice. However, normal folliculogenesis does require the AR, which suggests that androgen/AR signaling is also physiologically important in females (32).

To study how and why obesity develops in ARKO males, we began by examining the adrenal glands, which were hypertrophic in both males and females. In the present study, we explored the molecular basis of this observation. Dissection of the gland revealed that the layers of the zona fasciculata were thicker and coupled to the remaining layers of the X-zone (fetal zone). The hypertrophy resulted from a hypercorticoid state. Adrenal corticotropic hormone (ACTH) overproduction was driven by impaired negative feedback through the hypothalamus-pituitary-adrenal (HPA) axis. No clear alteration in the numbers of hormone-producing cells in the pituitary glands and hypothalamus was detected, but there were increased proopiomelanocortin (POMC) and decreased glucocorticoid

* Corresponding author. Mailing address: Institute of Molecular and Cellular Biosciences, University of Tokyo, 1-1-1 Yayoi, Bunkyo-ku, Tokyo 113-0032, Japan. Phone: 81-8-5841-8478. Fax: 81-3-5841-8477. E-mail: uskato@mail.ecc.u-tokyo.ac.jp.

† J.M. and T.M. contributed equally to this work.

▽ Published ahead of print on 30 April 2007.

receptor (GR) expression levels of transcripts in the ARKO pituitary glands. Androgen-induced GR gene activation was further confirmed in a pituitary gland-derived cell line (AtT-20 cells). These findings suggest that androgen/AR signaling in the pituitary gland supports the normal feedback system of glucocorticoid production through the HPA axis.

MATERIALS AND METHODS

Animals. ARKO mice were generated by targeted disruption of the AR gene by means of a Cre-loxP system (19) and maintained as described previously (16, 29, 30, 32). Experiments were performed with 2- to 25-week-old male mice. All mice protocols were approved by the Animal Care and Use Committee of the University of Tokyo (31, 40).

Cell culture. Adherent AtT-20 cells, a murine corticotropic tumor cell line, were cultured in a 5% CO_2 atmosphere at 37°C with Dulbecco's modified Eagle's medium-Ham's F12 at 1:1 containing 15% fetal calf serum (FCS) and penicillin-streptomycin. 3T3-L1 cells, a murine preadipocyte cell line, were cultured with Dulbecco's modified Eagle's medium containing 10% FCS. FCS in the culture media was replaced with charcoal-treated FCS for 1 week prior to the administration of 5α-dihydrotestosterone (DHT). For Northern and Western blot analyses, the cultured AtT-20 cells were subcultured in six-well plates. After incubation for 24 h, DHT (10^{-7} M) was added to the medium.

Histology and immunohistochemistry. Adrenal glands and pituitary glands were fixed by immersion with 4% paraformaldehyde for 24 h at 4°C. They were then embedded in paraffin, sliced into 4-μm sections by standard methods, and mounted onto silane-coated slides. After perfusion by 0.9% saline followed by 4% paraformaldehyde, brains were postfixed in the same fixative for 2 h at 4°C and soaked in phosphate-buffered saline containing 20% sucrose. Frontal sections were cut at 30-μm thickness using a cryostat. Serial sections were divided into four groups and used for single-labeling immunohistochemistry for the GR, corticotropin-releasing hormone (CRH), α-melanocyte-stimulating hormone (α-MSH), or thionin to allow determination of the areas to be measured.

Immunostaining was carried out using antibodies as described below (34). The primary antibodies included rabbit polyclonal anti-human AR (N-20; Santa Cruz Biotechnology, Santa Cruz, CA), rabbit polyclonal anti-GR (M-20; Santa Cruz Biotechnology, Santa Cruz, CA), mouse anti-human ACTH (DAKO, Carpinteria, CA), mouse anti-human luteinizing hormone β (Immunotech, Marseille, France), mouse anti-human follicle-stimulating hormone β (DAKO, Carpinteria, CA), mouse anti-human thyroid-stimulating hormone β (Advanced Immunochemical Inc., CA), rabbit anti-rat glycoprotein hormone (kindly supplied by A. F. Parlow, the National Institute of Diabetes and Digestive and Kidney Diseases [NIDDK], Bethesda, MD), rabbit anti-human growth hormone (DAKO, Carpinteria, CA), and rabbit anti-rat prolactin (kindly supplied by A. F. Parlow, NIDDK).

After treatment with 0.5% H_2O_2 (30 min) and 5% normal serum (1 h), the sections were incubated for 24 h at 4°C with specific primary antibodies. The sections were then incubated with secondary antibodies and an avidin-biotin complex (Vectastain ABC Elite kit; Vector Laboratories). The signals were visualized with diaminobenzidine and the nuclei were counterstained with hematoxylin.

For dual labeling of ACTH and the AR or GR, a single staining of the AR or GR was first performed as described above. After the primary antibodies were removed by treatment with 0.1 M glycine, sections were incubated with anti-ACTH antibodies followed by alkaline phosphatase-conjugated anti-mouse immunoglobulin G (DAKO, Carpinteria, CA). The signals were visualized with 5-bromo-4-chloro-3-indolyl-phosphate and nitroblue tetrazolium.

Detection of proliferation and apoptosis of adrenal gland cells. Eight-week-old mice were injected intraperitoneally (i.p.) with the thymidine analog 5'-bromo-2'-deoxyuridine (BrdU) (30 mg/g body weight [BW]) every 12 h five times (25). Mice were fully anesthetized and their adrenal glands removed 12 h after the last injection. Incorporated BrdU was detected immunohistochemically using a mouse monoclonal anti-BrdU antibody. The proliferative index was defined as the number of BrdU-positive cells per microscopic field. Five fields per mouse were counted for each of three wild-type (WT) and three ARKO mice.

Cells undergoing apoptosis were identified by digoxigenin labeling of the free 3'OH ends of fragmented DNA by use of terminal deoxynucleotidyltransferase (terminal deoxynucleotidyltransferase-mediated dUTP-biotin nick end labeling [TUNEL] assay). Assays were performed on sections from the same tissue blocks used for BrdU immunohistochemistry. Sections were counterstained with hematoxylin to facilitate cell counting. The fraction of apoptotic cells was defined as the fraction of diaminobenzidine-positive cells per total number of cells. Five fields per mouse were counted for each of three WT and three ARKO mice.

Serum endocrine parameters. A circadian rhythm experiment and dexamethasone suppression tests were performed on 8-week-old male mice as previously described (2). For the circadian rhythm experiment, blood was collected at 08:00 or 18:00 h. For the dexamethasone suppression tests, mice were injected i.p. with different doses of dexamethasone (0, 2, or 5 μg/20 g BW) in 0.3 ml of 0.9% saline. Injections were performed between 08:00 and 08:30 h and blood was collected 6 h later. Mice were fully anesthetized and blood was collected by cardiac puncture. Plasma ACTH and serum corticosterone were measured using radioimmunoassay kits (IRMA; Mitsubishi, Tokyo, Japan) at SRL (Tokyo, Japan), according to the manufacturers' instructions. Measurements were independently duplicated, and interassay variability and buffer dilution were corrected for by using internal correction factors.

RNA extraction and mRNA quantitation. Total mRNA was extracted from pituitary glands with TRIzol (Invitrogen) for reverse transcription-PCR (RT-PCR) and Northern blotting (35). To remove any possible DNA contamination prior to semiquantitative RT-PCR, the DNA was digested with RNase-free DNase. The digested total mRNA (2 μg) was subjected to RT using SuperScript reverse transcriptase (Invitrogen) primed by oligo(dT) primers. After first-strand cDNA synthesis, 1 ml from a 5% reaction mixture was diluted serially (2- to 128-fold). Amplification was performed with *rTaq*DNA polymerase (Takara) using primer pairs for GAPDH as an internal control to allow for concentration estimation (38). Expression levels of transcripts were measured using the standardized cDNA and specific primer pairs. The validity of the PCR products was confirmed by direct sequencing.

Western blot analysis. The lysates of mouse tissue and AtT-20 cells were resolved with sodium dodecyl sulfate-polyacrylamide gel electrophoresis and transferred onto nitrocellulose membranes (15, 39). Membranes were probed with rabbit polyclonal anti-GR antibody (M-20; Santa Cruz Biotechnology) and goat polyclonal anti-β-actin antibody (I-19; Santa Cruz Biotechnology) as an internal control. The blots were visualized using peroxidase-conjugated anti-rabbit antibody and anti-goat antibody, together with an ECL detection kit (Amersham Biosciences). The small interfering RNA analysis used AR and control small interfering RNA (Ambion), and transfection was accomplished with the Lipofectamine 2000 system (Invitrogen).

Luciferase reporter assay. GR promoter regions (upstream regions of exons 1B, 1C, and 2) were cloned by PCR and subcloned into a luciferase reporter gene driven by a tk promoter (tk-luc). PCR primers were as follows: for 1B Fw, 5'-GGCATAGTTAGGCCACTAAAGAGA-3'; for 1B Rv, 5'-GGGAGAAGT TGCAAAGCAGA-3'; for 1C Fw, 5'-CTGGAGCAGCAAATGTCAAG-3'; for 1C Rv, 5'-AGCTCGCAAAATGGAGGAG-3'; for 2 Fw, 5'-GGATCTGGCGT CCTTTTC-3'; and for 2 Rv, 5'-CCACATTATCTCTGATCCGATT-3'.

For the luciferase reporter assay, cultured cells were transfected with the indicated plasmids using the Lipofectamine Plus reagent (Invitrogen) into 24-well plates at 40 to 50% confluence. The total amount of DNA was adjusted by supplementing with empty vector up to 1.0 μg/well. Luciferase activity was determined using a dual luciferase assay system (Promega). As a reference plasmid to normalize the transfection efficiency, 1.5 ng/well of pRL-CMV plasmid (Promega) was cotransfected in all experiments.

Statistical analysis. Values are given as the means ± standard deviations. Comparisons between two groups were made by Student's *t* test. *P* values of <0.05 were accepted as statistically significant.

RESULTS

High serum levels of ACTH and corticosterone in male ARKO mice. The male ARKO ($AR^{L-/Y}$) mice exhibited growth retardation in comparison to WT male mice until 10 weeks of age but then showed catch-up growth over the next few weeks. Thereafter, the male ARKO mice weighed more than the WT mice and developed severe obesity (Fig. 1A) as previously reported (6, 30). Obesity to this extent was not seen for female ARKO ($AR^{L-/L-}$) mice. To identify causes for the late-onset obesity in male ARKO mice, serum endocrine parameters were measured. We found that serum corticosterone levels in male ARKO mice were elevated at 8 weeks of age and became significantly higher at 13 and 20 weeks ($P < 0.05$ and $P < 0.01$, respectively) (Fig. 1B).

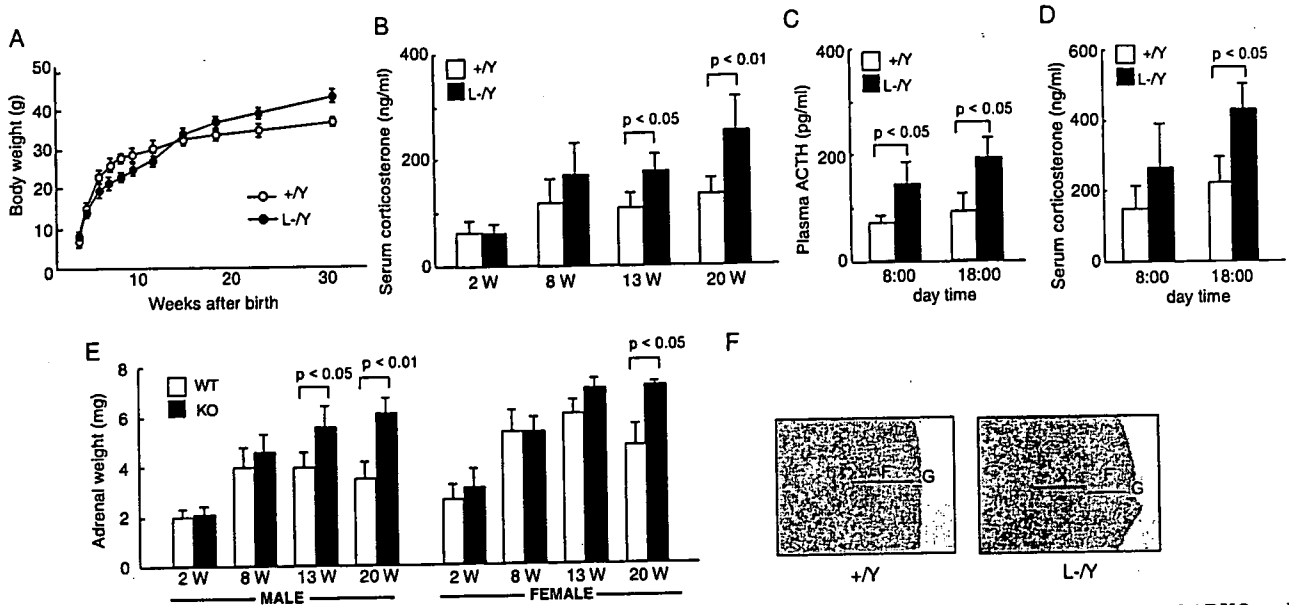

FIG. 1. Hypertrophic adrenal glands with high serum levels of ACTH and corticosterone in ARKO mice. (A) Growth curves of ARKO and WT littermate mice. The floxed AR mice (female, $AR^{L+/L+}$; male, $AR^{L+/Y}$) were crossed with Cre-CMV transgenic mice to generate ARKO male ($AR^{L-/Y}$) and female ($AR^{L-/L-}$) mice (16, 30). (B) Serum corticosterone levels of ARKO and WT mice at 2, 8, 13, and 20 weeks (W) of age. (C) Plasma ACTH levels of ARKO and WT mice measured in the morning (8:00) and evening (18:00). (D) Serum corticosterone levels of ARKO and WT mice in the morning (8:00) and evening (18:00). (E) Adrenal gland weights of male and female ARKO and WT mice at 2, 8, 13, and 20 weeks of age. (F) Histology of ARKO and WT adrenal glands. All sections were stained with hematoxylin and eosin. F, zona fasciculata; G, zona glomerulosa; X, X-zone.

To more carefully examine the hypercorticoid state in male ARKO mice, we measured the serum levels of corticosterone and its upstream hormone ACTH. Measurements were taken both in the morning and in the evening, as these hormones exhibit a circadian rhythm. As expected, the 8-week-old WT and ARKO mice had low levels of both hormones in the morning and higher levels in the evening (Fig. 1C and D). Overall, the ARKO males tended to have high levels of ACTH and corticosterone at any time compared to WT mice. They had significantly high levels of plasma ACTH at both 8:00 and 18:00 and high levels of corticosterone at 18:00 compared to WT mice ($P < 0.05$) (Fig. 1C and D). However, for female ARKO mice, though serum levels of these hormones tended to be higher than in WT littermates, the differences were not statistically significant (data not shown). The obesity seen for these mice was likely the result of their hypercorticoid state, as centripetal obesity is a typical symptom of Cushing's syndrome. In the following experiments, we explored the etiology of the hypercorticoid state in the ARKO mice.

Hypertrophic adrenal glands in ARKO mice. To investigate the hypercorticoid state in the ARKO mice, we first examined the adrenal glands. The adrenal glands in the ARKO males clearly weighed more than the glands of WT mice at 13 weeks of age (Fig. 1E). This coincided with the onset of obesity and the hypercorticoid state. Likewise, in ARKO females, the adrenal glands also increased in size in comparison to what was seen for WT littermate females; however, the growth was not as pronounced as that in ARKO males (Fig. 1E). The adrenal glands of male ARKO mice were then used for subsequent experiments.

The adrenal cortex forms the major part of the gland and is divided into three layers in mammals: the zona glomerulosa, immediately beneath the capsule, followed by the zona fasciculata and the zona reticularis. The zona reticularis is replaced in rodents by the X-zone, which develops prenatally and begins to degenerate at pubertal maturity in males. In mice, corticosterone, the major glucocorticoid in rodents, is produced in the zona fasciculata, while aldosterone, the most potent mineralocorticoid, is formed in the zona glomerulosa. Hematoxylin and eosin staining of adrenal glands in 13-week-old mice revealed that the enlargement of the adrenal glands in ARKO males was caused by cellular hypertrophy of the zona fasciculata as well as by a failure of X-zone (fetal zone) regression (Fig. 1F). Since glucocorticoids are produced in the zona fasciculata, it is likely that the overproduction of corticosterone is the result of the hypertrophy in this area.

Increased proliferation and decreased apoptosis in the adrenal cortex of ARKO males. The failed regression of the X-zone in 13-week-old ARKO males raised the possibility of impaired cell death or decreased apoptosis in the adrenal cortex. Indeed, the percentage of apoptotic cells in the zona fasciculata, detected by TUNEL assay in the ARKO males, was clearly less (19.5%) than that for WT mice (33.1%) (Fig. 2A). When actively proliferating cells of the adrenal glands were counted by BrdU labeling in WT and ARKO males, 2.5 times more BrdU-labeled cells/section were found in ARKO mice. This suggests increased proliferation in the adrenal cortex of ARKO mice (Fig. 2B). Thus, the hypercorticoid state likely results from the overproduction of glucocorticoid by the hypertrophic zona fasciculata. This hypertrophy is caused by chronic exposure to high levels of ACTH.

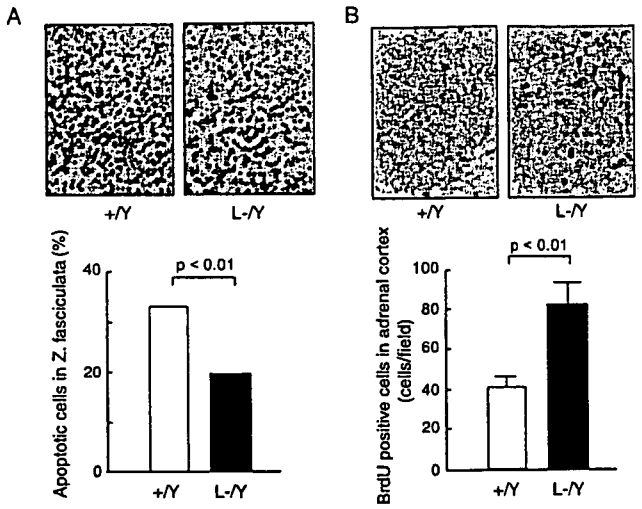

FIG. 2. Increased proliferation and decreased apoptosis in ARKO adrenal glands. (A) Decreased apoptosis in the ARKO adrenal glands. Histogram showing the number of TUNEL-positive cells in the zona fasciculata (Z. fasciculata). (B) Increased proliferation in the ARKO adrenal cortex. Histogram showing the number of BrdU-positive cells.

The HPA negative feedback system for glucocorticoid production is impaired in ARKO males. Glucocorticoid synthesis is regulated by a negative feedback loop via the HPA axis involving CRH and ACTH, produced by the hypothalamus and pituitary glands, respectively. We assessed whether the axis was intact and functioning normally in the ARKO males with a dexamethasone suppression test. As expected, serum corticosterone levels were down-regulated in 8-week-old WT mice 6 hours after i.p. injection of either 2 μg/20 g BW or 5 μg/20 g BW of dexamethasone (Fig. 3A). In ARKO mice, injection with 2 μg/20 g BW of dexamethasone did not suppress the serum levels of corticosterone. However, a dose of 5 μg/20 g BW was effective in lowering the serum levels of corticosterone in ARKO mice (Fig. 3A). This is similar to the high-dose dexamethasone suppression seen for patients with central Cushing's syndrome. Plasma ACTH levels in both the ARKO and WT males were decreased 6 h after dexamethasone injection at both the low and high doses; however, suppression was less sensitive in the ARKO males than in the WT males (Fig. 3B). No statistical difference in ACTH levels was detected between ARKO and WT males in this suppression test.

No overt abnormalities were present in the hypothalami or pituitary glands of ARKO males. The results of the suppression tests suggested that the adrenal hypertrophy of the ARKO males resulted from the hyperfunction of the hypothalami and/or pituitary glands. To address this issue, the hypothalami and pituitary glands of 8-week-old ARKO males were histologically examined. No overt abnormalities were detected in sections of the ARKO mice stained with hematoxylin and eosin (Fig. 4A). Immunohistochemical staining of the pituitary glands demonstrated similar numbers of cells expressing pituitary hormones in WT and ARKO mice (Fig. 4B). AR protein expression was detectable in several types of hormone-producing cells in the WT males but was absent in the ARKO mice (data not shown).

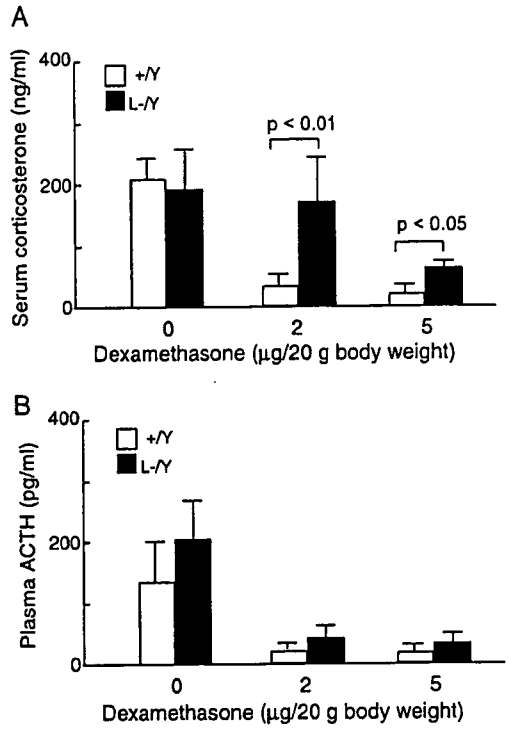

FIG. 3. Impairment of the HPA negative feedback system of glucocorticoid production in ARKO mice. (A) Serum corticosterone levels of ARKO and WT mice in the dexamethasone suppression test. Trunk blood was collected from ARKO and WT mice 6 hours after injection with increasing doses of dexamethasone. (B) Plasma ACTH levels of ARKO and WT mice in the dexamethasone suppression test.

Increased POMC expression and decreased GR expression in the pituitary glands is caused by AR deficiency. To address if hormone production was intact following AR inactivation, we examined the mRNA expression levels of pituitary hormones by RT-PCR. As shown in Fig. 5A, the expression of luteinizing hormone β, follicle-stimulating hormone β, and thyroid-stimulating hormone β, as well as that of the orphan NRs (Nur77 and Nurr1), appeared unaltered by AR deficiency. The POMC mRNA levels, however, were clearly up-regulated in males (Fig. 5A) but not in females (Fig. 5B). The up-regulation of POMC mRNA was confirmed by Northern blot analysis (Fig. 5C). This finding is consistent with the high ACTH levels observed for the ARKO mice. In contrast, pituitary GR expression was decreased at both the mRNA and protein levels (Fig. 5A and D). Decreased GR gene expression in ARKO males was also seen for the spleen but not for the other tested tissues (Fig. 5E), suggesting tissue-specific regulation of GR expression by the AR. Interestingly, a clear decrease in the GR mRNA levels was not detected in the total brain RNA of ARKO males (Fig. 5E). Additionally, there was no alteration in the numbers of GR and CRH immunoreactive cells in the hypothalamic paraventricular nucleus in the male ARKO brain (Fig. 4D). These results suggest that the androgen/AR signaling system affects the negative feedback regulation of glucocorticoid production via pituitary GR expression. This view is further supported by the observation that colocalization of ACTH with the AR and/or GR in the pituitary

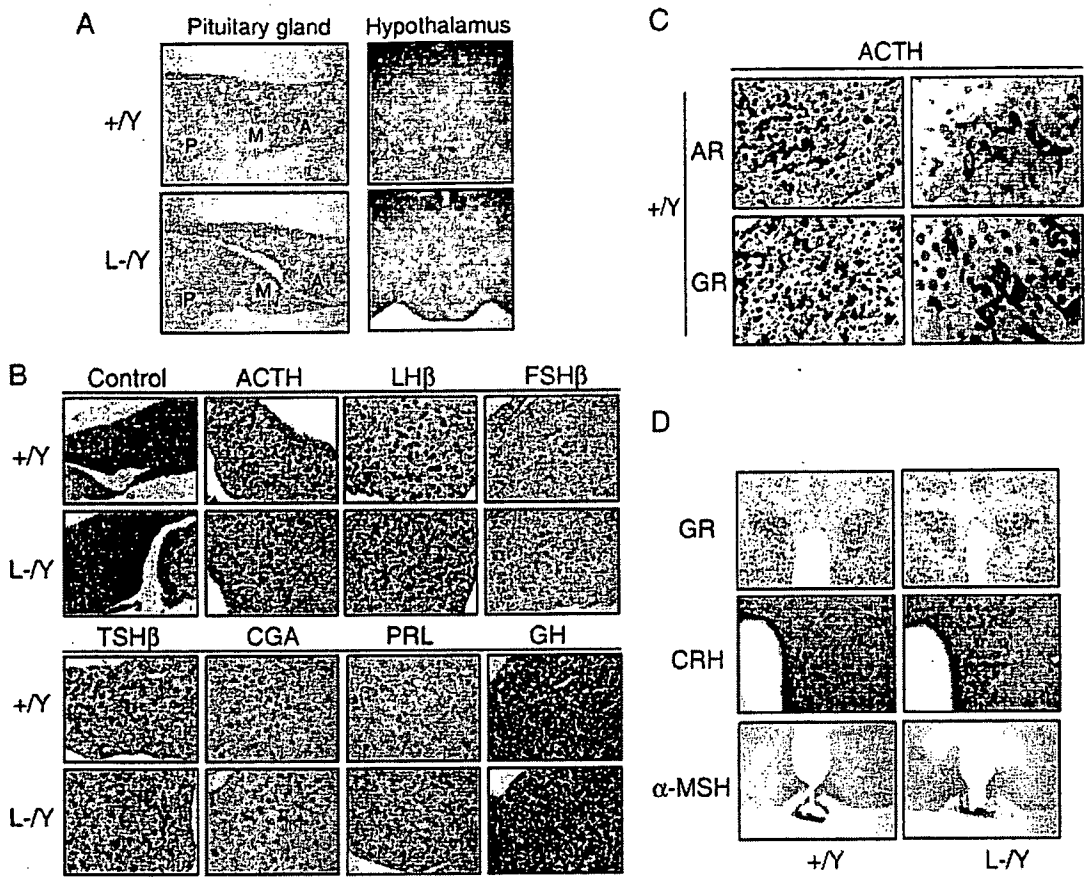

FIG. 4. Histological appearance of the hypothalamus and pituitary gland in ARKO mice. (A) No clear alteration in morphology of the hypothalami or pituitary glands of ARKO mice. Sections of pituitary glands and hypothalami were stained with hematoxylin and eosin. A, anterior lobe; M, intermediate lobe; P, posterior lobe. (B) No overt abnormality in the distribution of cells expressing pituitary hormones in ARKO mice by immunohistochemical staining. LHβ, luteinizing hormone β; FSHβ, follicle-stimulating hormone β; TSHβ, thyroid-stimulating hormone β; CGA, glycoprotein hormone; PRL, prolactin; GH, growth hormone. (C) Pituitary ACTH (black/gray) colocalized with AR (brown) or GR (brown) (left) and its higher magnification (right) in WT mice as detected by immunostaining with specific antibodies. (D) No clear alterations in the GR and CRH (in the paraventricular nucleus) and α-MSH (in the arcuate nucleus) immunoreactive neurons in the hypothalami of ARKO mice.

glands of WT mice was detected by double immunostaining with specific antibodies (Fig. 4C).

Induction of the GR gene by DHT in a pituitary cell line. Finally, to confirm that GR expression levels in the pituitary glands of ARKO mice were reduced, we tested whether DHT induced GR gene expression in cultured cells. DHT treatment of the pituitary cell line AtT-20 for 4 h induced expression of the GR gene (Fig. 6A) and protein (Fig. 6B). Unexpectedly, the expression levels of POMC mRNA (Fig. 6A) and protein (Fig. 6B) were reduced. The AR effect was confirmed following treatment with an AR antagonist (Flutamide) (Fig. 6A and B) and RNA interference (Fig. 6C). Reflecting tissue-specific regulation of GR expression by the AR in intact animals, no response to DHT in the expression levels of either GR or POMC was seen in 3T3-L1 preadipocytes (Fig. 6A to C, lower panels). No consensus androgen response elements or closely related sequences are present up to −3 kb in the GR promoter. However, the intron between exons 1A and 1B of the GR gene (33) was found to counter androgen responsiveness in a transient expression assay in AtT-20 cells (Fig. 6D). This suggests that this element is responsible for androgen-induced GR expression in the pituitary.

DISCUSSION

Hypertrophic and hyperplastic adrenal glands are associated with a hypercorticoid state in male mice deficient for the AR. A hypercorticoid state was observed in sexually mature male mice deficient for the AR. It likely resulted from glucocorticoid overproduction by the hypertrophic and hyperplastic zona fasciculata of the adrenal gland. The ARKO mice demonstrated hyperplasia of the X-zone, which normally regresses by the time sexual maturity is attained (11). TUNEL assays and BrdU labeling confirmed that the hypertrophy and hyperplasia of adrenal glands resulted from decreased apoptosis and increased cell proliferation. Chronic ACTH stimulation causes zona fasciculata cell hypertrophy and hyperplasia, and ACTH is a potent inhibitor of apoptosis in the adrenal cortex (36). Thus, the findings for the ARKO males are consistent with exposure to high levels of ACTH.